

Optimal Targeting in Dynamic Systems

Yuchen Hu
MIT

Shuangning Li
University of Chicago

Stefan Wager
Stanford University

Draft version July 2025

Abstract

Modern treatment targeting methods often rely on estimating the conditional average treatment effect (CATE) using machine learning tools. While effective in identifying who benefits from treatment on the individual level, these approaches typically overlook system-level dynamics that may arise when treatments induce strain on shared capacity. We study the problem of targeting in Markovian systems, where treatment decisions must be made one at a time as units arrive, and early decisions can impact later outcomes through delayed or limited access to resources. We show that optimal policies in such settings compare CATE-like quantities to state-specific thresholds, where each threshold reflects the expected cumulative impact on the system of treating an additional individual in the given state. We propose an algorithm that augments standard CATE estimation with off-policy evaluation techniques to estimate these thresholds from observational data. Theoretical results establish consistency and convergence guarantees, and empirical studies demonstrate that our method improves long-run outcomes considerably relative to individual-level CATE targeting rules.

1 Introduction

Flexible machine-learning-based causal inference tools are widely used to guide decision-making and treatment prioritization rules across various domains. The conditional average treatment effect (CATE), which quantifies the expected benefit of treatment conditionally on individual characteristics, serves as a key metric for characterizing treatment heterogeneity and identifying units most likely to benefit from treatment [Athey and Imbens, 2016]. Many machine learning models have been developed and applied to estimate CATE using rich sets of features. For example, using electronic health records, Zainal et al. [2024] have found that the causal forest algorithm [Athey et al., 2019] can identify some groups of patients with depression and suicidal ideation who strongly benefit from psychiatric hospitalization, and other groups of patients who may even respond negatively to hospitalization.

One practical limitation of these machine-learning-based approaches is that they usually focus only on understanding, on a unit-by-unit level, who would benefit from receiving a treatment. However, if an organization such as the Veterans Health Administration wanted to operationalize the findings from these approaches, they would also need to consider how the resulting policy might stress their available resources and infrastructure [Hussey et al., 2016]. In the short-to-medium term, the number of available hospital beds is likely a fixed resource, so beyond a certain point, assigning more patients to inpatient care may cause delays or reduce resource availability for other patients.

The goal of this work is to augment machine-learning-based methods for optimal targeting, such as causal forests, to make them aware of (and responsive to) capacity constraints induced by the system’s dynamics that may stochastically limit or delay the number of units that can receive treatment at any given time. We believe this to be a problem setting with broad applicability. For example, such methods could be used for targeting expedited delivery in online delivery platforms or fast-track care in the emergency department. In order to address long wait times in emergency departments, some hospitals implement fast-track systems to divert patients with more minor illnesses from the main intake system and enable them to get faster care [Meislin et al., 1988]. Using a machine learning system to target assignment to the fast-track system could be promising; however, any such system should also be aware of the current queuing conditions and capacity resources of the hospital.

The problem of optimal treatment assignment in a dynamic system is a reinforcement learning problem—and, when working with complex or high-dimensional inputs as are often encountered with, e.g., electronic health records, one might expect this reinforcement learning problem to be intractably complicated. We find, however, our optimal targeting problem admits a simple and intuitive solution: We show that policymakers can account for treatment-induced congestion effects by combining standard treatment prioritization rules with state-dependent decision thresholds.

More specifically, using the hospital admission setting as a motivating example, let $\tau(x, k)$ represent the direct effect of hospitalization for patients with health records x given the level of system congestion k ; following Munro et al. [2025], we refer to this quantity as conditional average direct effect (CADE). Then, our results show that the optimal policy must take the form of a CADE-thresholding rule with state-specific thresholds c_k , and assigns treatment only to those whose health records X_i satisfy $\tau(X_i, k) > c_k$. This structure closely mirrors that of optimal treatment prioritization rules under static budget constraints [Bhattacharya and Dupas, 2012, Sun et al., 2021]. The relationship between these thresholds c_k , as well as their magnitude, is shaped by the intricate interplay of the system’s dynamics, the distribution of covariates, and the outcome function, each of which can vary largely depending on the context. Yet, despite this complexity, we show that it is possible to estimate these threshold values from a single observational dataset using off-policy evaluation methods. In doing so, treatment decisions can be fine-tuned to strike a balance between individual benefit and system capacity.

1.1 Related Work

The problem of learning optimal targeting rules has been extensively studied over the past two decades, primarily in settings where treatment assignments are considered independently across units [Manski, 2004, 2009, Hirano and Porter, 2009, Stoye, 2009, 2012, Qian and Murphy, 2011, Kitagawa and Tetenov, 2018, Kallus, 2018, Luedtke and Chambaz, 2020, Athey and Wager, 2021]. Works in this vein have then focused on deriving regret-optimal treatment rules in heterogeneous populations that depend solely on the focal unit’s condition. In such settings, recent advances in machine learning have allowed for accounting for heterogeneous treatment effects based on a rich set of covariates [Chernozhukov et al., 2018, 2022, Wager and Athey, 2018, Athey et al., 2019, Nie and Wager, 2021, Athey and Wager, 2021, Farrell et al., 2021]. Our approach differs from those by considering the potential interactions between different treatment assignments that arise from a shared pool of limited resources, particularly in the form of stochastic delay or congestion.

Our work deals with dynamic capacity constraints limiting the number of units eligible

for treatment. From this perspective, our research is related to the strand of literature on finding optimal targeting rules under budget constraints [Bhattacharya and Dupas, 2012, Luedtke and van der Laan, 2016, Le et al., 2019, Wang et al., 2018, Xu et al., 2022, Huang and Xu, 2020, Sun, 2021, Kitagawa and Wang, 2023b, Zhou et al., 2023, Imai and Li, 2023, Yadlowsky et al., 2025, Sun et al., 2021, Sverdrup et al., 2024]. However, these works typically assume a fixed, one-time budget—where resources are permanently depleted once allocated—whereas our approach considers dynamic resource capacity, which can recover as units are served and exit the system.

Shared capacity or state can be understood as a form of interference, where the treatment assigned to units arriving earlier may affect the outcomes of units arriving later. While there is a growing body of literature studies the estimation of treatment effects under interference within the Neyman–Rubin framework [Hudgens and Halloran, 2008, Tchetgen Tchetgen and VanderWeele, 2012, Manski, 2013, Aronow and Samii, 2017, Basse et al., 2019, Li and Wager, 2020, Leung, 2022, Farias et al., 2022, Sävje et al., 2021, Zhan et al., 2024, Johari et al., 2024], including the recent works that study causal inference and experimentation under stochastic congestion [Li et al., 2023, Boutilier et al., 2024], few studies have focused on optimal targeting under such conditions. Existing works in this area tend to address the challenge by determining a single treatment assignment rule for the entire population at once [Viviano, 2024, Galeotti et al., 2020, Munro et al., 2025, Kitagawa and Wang, 2023a,b, Zhang and Imai, 2023], whereas the problem we consider involves sequential targeting, where decisions are made one at a time as units arrive in the system. The targeting threshold in our framework is conceptually related to the conditional average indirect effect studied in Munro et al. [2025], which extends the average indirect effect studied in Hu et al. [2022] and Li and Wager [2020]. However, unlike those works, our method does not require explicitly estimating this effect through augmented experiments with perturbations. Instead, we regard the threshold as a tuning parameter, which can be optimized using metrics derived from off-policy evaluation methods.

Our work is also closely related to the literature on off-policy learning in dynamic processes. Early contributions in this field primarily focused on learning a sequence of treatment rules that depend on the entire history of the process [Murphy, 2003, 2005, Robins, 2004, Zhang et al., 2013, Nie et al., 2021]. This approach imposes restrictions on both the total number of periods and the complexity of the historical information being tracked. In the average reward setting that we consider [Howard, 1960], a more common approach is to model the system as a Markov decision process, and approximate the optimal treatment policy using either gradient-based methods [Sutton et al., 1999, Zhang and Ross, 2021, Kallus and Zhou, 2021] or grid search with off-policy evaluation methods [Liao et al., 2021, 2022, Kallus and Uehara, 2020, 2022]. A key distinction between the Markov model we use and those commonly found in the literature is the handling of covariates. We assume that the units’ covariates are fully exogenous, which allows us to separate individual-level characteristics tied to a unit’s own treatment experience from the system-level state that passes down through the system and affects future units. In contrast, typical MDP models often blur this distinction between individual covariates and system states, which can lead to unnecessarily complex dynamics and inflated policy spaces.

A particularly relevant line of work is the literature on exogenous Markov decision processes [Dietterich et al., 2018, Efroni et al., 2022, Sinclair et al., 2023, Wan et al., 2024]. In an exogenous MDP, the state is partitioned into an endogenous component and an exogenous component, where the latter evolves independently of the decision maker’s actions. Work there then primarily focuses on leveraging this structure to improve the performance

of reinforcement learning algorithms. Our framework can be viewed as a special case of an exogenous MDP, where the covariate plays the role of the exogenous state. However, we further restrict the impact of the covariate on the endogenous state, which enables a simplified form for the optimal targeting rule and reveals connections to treatment prioritization strategies commonly used in practice.

Finally, at a higher level, the problem we aim to address is closely related to those studied in the dynamic resource allocation and optimal control literature (e.g., Naor [1969], Johansen and Stidham Jr [1980], Chen and Frank [2001], Borgs et al. [2014], Xu and Chan [2016], Agrawal and Jia [2019], Cheung and Simchi-Levi [2019], Murthy et al. [2022], Chen et al. [2024], Boutilier et al. [2024] and references therein). Much of this literature has focused on managing limited capacity with system-level objectives and often abstracts away individual-level heterogeneity. More recently, there has been a growing interest in data-driven approaches that leverage covariate or contextual information to improve decision-making in revenue and inventory management [Feng and Shanthikumar, 2018, Ban and Rudin, 2019, Bertsimas and Kallus, 2020, Chen et al., 2022, Ding et al., 2024], as well as in patient prioritization and triage [Jacobson et al., 2012, Mills et al., 2013, Shi et al., 2024, Keskin and Zhang, 2024]. Our work contributes to this literature by introducing a perspective that bridges causal machine learning tools with dynamic constraints, which enables simple, interpretable decision making even in the presence of complex covariates.

2 Targeting in Dynamic Systems

Consider the problem of targeting in a single dynamic system, where units $i = 1, \dots, n$ arrive sequentially. When each unit i arrives, we observe their covariate $X_i \in \mathcal{X}$ and decide on a treatment $W_i \in \{0, 1\}$ to assign. Each time a unit arrives and is assigned a treatment, this may alter the system’s dynamics. We capture this dynamic feature using the state variable $S_i \in \mathcal{S}$, which represents the system’s condition at the time of the unit’s arrival. The unit’s outcome, $Y_i \in \mathbb{R}$, may depend on their covariate X_i , the treatment assignment W_i , and the current state S_i . Let $\pi : \mathcal{X} \times \mathcal{S} \rightarrow [0, 1]$ denote the treatment assignment policy, i.e., $\mathbb{P}[W_i = 1 \mid X_i = x, S_i = s] = \pi(x, s)$ under policy π . We assume the outcome is a proxy of utility and are interested in learning a good policy π from an observed dataset of size n that maximizes the average outcome.

Example 1 (Routing Customer Support Requests). In an online service platform, customer support tickets arrive sequentially, each with observed features X_i such as account information and request details. The platform decides whether to route the ticket to a specialist ($W_i = 1$) or assign it to regular support staff which is not capacity-constrained ($W_i = 0$). The system state S_i represents the number of unresolved tickets awaiting specialist attention. The customer’s satisfaction score may depend on the assignment, their features, and specialist queue length if routed to them.

Example 2 (Emergency Department Triage). In a hospital emergency department, patients arrive sequentially, each with observed clinical features X_i . The hospital needs to decide whether to offer fast-track treatment ($W_i = 1$) or place the patient in the regular queue ($W_i = 0$). The system state S_i reflects the numbers of patients currently in the fast-track and regular queues. The patient’s health outcome may depend on both their clinical features and the queue length of the queue they are assigned to.

One common targeting strategy is to estimate the conditional average treatment effect (CATE) from a sample of n units, and implement a policy that targets all units with a positive estimated CATE [Stoye, 2012, Tetenov, 2012]. We refer to this targeting strategy as the direct targeting rule, as it targets individuals based on the direct effect of the treatment on that individual.

Definition 1 (Direct Targeting Rule). Let $\tau(x, s)$ be the state-aware conditional average treatment effect:

$$\tau(x, s) := \mathbb{E}[Y_i \mid X_i = x, S_i = s, W_i = 1] - \mathbb{E}[Y_i \mid X_i = x, S_i = s, W_i = 0], \quad (1)$$

and $\hat{\tau}(x, s)$ be an estimated conditional average treatment effect from the dataset. The direct targeting rule π^d assigns treatment whenever $\hat{\tau}(x, s) > 0$, i.e., $\pi^d(x, s) = I(\hat{\tau}(x, s) > 0)$.

One might think that this targeting strategy already accounts for the dynamic nature of the system, since the state variable S_i is also used for targeting. For example, if the treatment represents admission to a system and the state variable represents the busyness level of the system, the direct targeting rule might only assign individuals to the system when it is not busy. However, this argument overlooks how the treatment assignment might affect the system state. Under a direct targeting rule, individuals who benefit only marginally from treatment may still join the system, potentially causing congestion that crowds out individuals for whom treatment would have had substantial benefit. In fact, as we will show later, the direct targeting rule may only be optimal when the treatment assignment has little impact on state evolution, or when the all units are insensitive to the system's state.

We first make the following assumptions about the stability of the system, which allow us to formally define an optimal policy in a dynamic system.

Assumption 1 (Time-Homogenous MDP with Exogenous Covariates). The system transition is governed by a set of time-homogenous distributions $\{P_X(\cdot), P_Y(\cdot \mid x, s, w), P_S(\cdot \mid s, w)\}$ such that, for all units i and conditionally on the past, X_i , Y_i and S_{i+1} are drawn according to the densities $P_X(\cdot)$, $P_Y(\cdot \mid X_i, S_i, W_i)$ and $P_S(\cdot \mid S_i, W_i)$.

Assumption 2 (Irreducibility and Boundedness). The process $\{S_i \mid i = 1, 2, \dots\}$ induced by any policy π is irreducible and aperiodic. Furthermore, the state space \mathcal{S} is finite, and the outcomes Y_i are uniformly bounded almost surely.

A representation of such a Markov decision process with exogenous covariates can be found in Figure 1. In Section 3, we provide a concrete example of how this framework naturally models a large class of queuing systems. Assumptions 1 and 2 ensure that there exists a unique stationary distribution of the state (denoted as d_π), and the average outcome under the policy π exists and can be reduced to the following form that does not rely on the initial state:

$$\lim_{n \rightarrow \infty} \mathbb{E} \left[\frac{1}{n} \sum_{i=1}^n Y_i \mid S_1 = s \right] = \mathbb{E}_\pi[Y_i] =: \mu(\pi), \quad (2)$$

where the expectation is taken over the joint distribution of P_Y , P_X , and the stationary distribution d_π , i.e., $\mathbb{E}_\pi[Y_i] = \int_{\mathcal{X}} \sum_{s \in \mathcal{S}} P_X(x) d_\pi(s) \mathbb{E}_\pi[Y_i \mid S_i = s, X_i = x] dx$ [Van Roy, 1998]. We say that a policy is optimal if it maximizes the average outcome $\mu(\pi)$.

Definition 2 (Optimal Targeting Rule). A targeting rule $\pi^* : \mathcal{X} \times \mathcal{S} \rightarrow [0, 1]$ is optimal if

$$\pi^* \in \arg \max_{\pi} \mu(\pi). \quad (3)$$

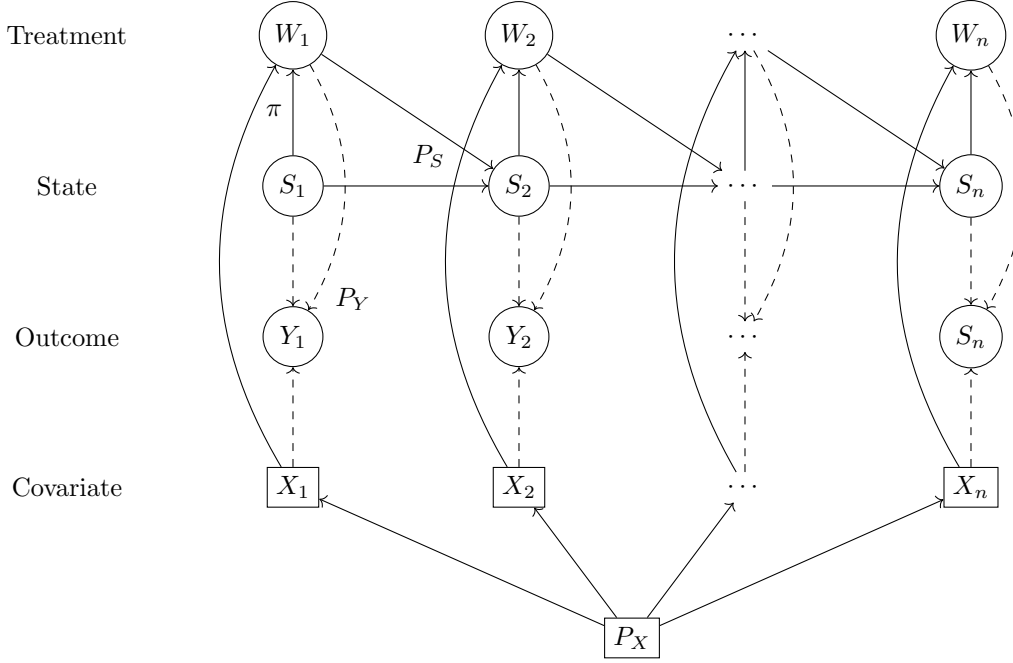


Figure 1: An illustration of a sample of size n drawn from a time-homogeneous Markov decision process with exogenous covariates.

2.1 A First-Order Characterization of Optimal Treatment Rules

Our approach to optimal targeting starts by considering the policy gradient, which quantifies how changes in the policy (i.e., treatment-assignment policies) affect the expected outcome. We define the conditional policy gradient $H(x, s; \pi)$ as the benefit from increasing treatment intensity for units with covariate $X_i = x$ arriving when the system is in state $S_i = s$:

$$H(x, s; \pi) = \frac{1}{P_X(x) \cdot d_\pi(s)} \frac{\partial}{\partial \pi(x, s)} \mu(\pi). \quad (4)$$

We note that $H(x, s; \pi)$ may also be interpreted as the conditional total effect of assigning treatment to units with covariate x in state s [Hu et al., 2022].¹ Clearly, at the optimal policy π^* must be unimprovable by policy-gradient ascent; and our first main result (Theorem 2) will use this fact to provide a useful characterization of the form of π^* .

We start by decomposing the conditional policy gradient $H(x, s; \pi)$ into a Conditional Average Direct Effect (CADE) of the treatment on the unit itself, and a Conditional Average Indirect Effect (CAIE) on all subsequent arrivals. The proof is similar to that of the policy gradient theorem in an average-reward setting.

Proposition 1. *Under Assumptions 1 and 2, the conditional policy gradient can be decom-*

¹We divide the policy gradient by $P_X(x) \cdot d_\pi(s)$, the probability of observing the covariate-state pair (x, s) , to isolate the conditional impact of adjusting the policy specifically for units with covariate x in state s .

posed as

$$H(x, s; \pi) = \underbrace{\tau(x, s)}_{\text{CADE}} + \underbrace{C_\pi(s)}_{\text{CAIE}}, \quad (5)$$

where

$$\begin{aligned} C_\pi(s) = & \lim_{n \rightarrow \infty} \mathbb{E}_\pi \left[\sum_{i=2}^n (Y_i - \mu(\pi)) \mid S_1 = s, W_1 = 1 \right] \\ & - \lim_{n \rightarrow \infty} \mathbb{E}_\pi \left[\sum_{i=2}^n (Y_i - \mu(\pi)) \mid S_1 = s, W_1 = 0 \right]. \end{aligned} \quad (6)$$

We note that the CADE shares the same form as the CATE defined in Definition 1 that has been widely studied in the literature: When the system state S_i is drawn i.i.d. from some distribution, there is no interference across units, and the CADE coincides with the CATE.² However, when the system states are temporally linked as in our setting, $\tau(x, s)$ no longer captures the total conditional average effect of a treatment assignment, and instead represents only its direct impact. To fully characterize the consequences of a treatment, one must additionally account for the CAIE. A key insight from Proposition 1 is that the CAIE depends only on the state s , not on the covariate x . As we will discuss later, this insight forms the foundation for our targeting policy, which searches over $|\mathcal{S}|$ threshold values.

Proposition 1 can be naturally utilized to compute the gradient in a policy gradient algorithm. Since the Markov chain is stationary with a finite state space, the local gradient evaluated at the status quo policy μ_0 can be obtained by computing the CADE and the CAIE using the observed dataset under μ_0 . If repeated experimentation is feasible, one may then iteratively compute the gradient at the current policy and update accordingly until convergence to find the optimal targeting rule; such iterative policy updating is a standard use of policy gradients in the reinforcement learning literature [Sutton et al., 1999].

In our setting, however, Proposition 1 offers more than just a means for computing a gradient for the purpose of iterative policy improvement. As we show below, the decomposition sheds light on a simple structural form of the optimal targeting rule, which substantially reduces the complexity of the policy class and enables off-policy learning with a single observational dataset. In many applications—such as targeting fast-track care in emergency departments—repeated experimentation may not always be possible, and one must rely on a single offline dataset. In such cases, our results enable off-policy learning under realistic data collection constraints.

Theorem 2. *Under the conditions of Proposition 1, there exists an optimal policy of the form*

$$\pi^*(x, s) = I(\tau(x, s) > c_s) + I(\tau(x, s) = c_s) \cdot p_s \quad (7)$$

for some constant $c_s \in \mathbb{R}$ and $p_s \in [0, 1]$, $\forall x \in \mathcal{X}, s \in \mathcal{S}$. Furthermore, if the direct effect $\tau(X, s)$ is continuously distributed for all s , there exists an optimal policy of the form

$$\pi^*(x, s) = I(\tau(x, s) > c_s). \quad (8)$$

²This phenomenon, i.e., that the average direct effect of a treatment in a system with spillovers matches the average treatment effect in a system where spillovers are suppressed, has also been observed in many different models [e.g., Sävje et al., 2021, Munro et al., 2025].

Theorem 2 implies that, to identify the optimal policy, it suffices to consider only policies that compare the direct effect $\tau(x, s)$ with a state-specific threshold. For example, if the dynamic system of interest is a queuing system, Theorem 2 suggests that the optimal policy should apply a different threshold for treating patients at each queue length. This threshold represents the expected cumulative negative impact due to delays from treating an additional patient at that queue length under the optimal policy. Estimating this negative impact is challenging with a single offline dataset, as it must be evaluated under the unknown optimal policy. However, in Section 2.2, we present an algorithm that searches over a grid of quantiles of $\hat{\tau}(X, s)$ using off-policy evaluation methods, which allows for effective targeting using a single offline dataset.

We note that this conditional policy gradient approach strictly generalizes the standard CATE-based targeting rule in Definition 1. In the classical setting, where the treatment does not affect the system’s dynamics, the indirect effect $C_\pi(s)$ is always zero. Thus, the gradient of any policy π is simply $\tau(x, s)$, in which case the maximum is always taken at the endpoints, with $\pi^*(x, s) = I(\tau(x, s) > 0)$.

When $\tau(X, s)$ remains a continuous random variable for all fixed s , which ensures that the probability for two units having the same direct treatment effect is zero, the optimal policy reduces to a simple deterministic form. One sufficient condition for this to hold is that the covariate X_i has a continuous component, and the mapping $\tau(x, \cdot)$ is also continuous in x . In settings where x represents a rich set of features, such as electronic health records or a digital footprint, and where $\tau(x, \cdot)$ cannot be reduced to a linear combination of indicator functions in x , this assumption would be satisfied.

Remark 1. An alternative model of the system is to collapse X_i and S_i into a large state variable, which allows for richer interaction between the covariate and the state transition. This recovers the standard off-policy learning problem in MDPs [Sutton and Barto, 2018], where the policy space is now as large as $\mathcal{O}(|\mathcal{X} \times \mathcal{S}|)$, and learning the optimal policy requires specifying the treatment assignment probability for all pairs (x, s) . One could still, in principle, estimate the value $\mu(\pi)$ for all feasible policies π and select the policy with the highest estimated value. However, since the covariate x may encode high-dimensional or complex features, the resulting policy class is typically too large for direct off-policy learning to be practical without strong structural assumptions or parametric restrictions. In contrast, our result reduces the policy search to just $\mathcal{O}(|\mathcal{S}|)$ thresholds,³ which substantially simplifies the learning problem and enables tractable off-policy optimization even with rich covariates.

2.2 A State-Aware Targeting Algorithm

Theorem 2 suggests a straightforward approach for identifying optimal targeting policies:

1. Estimate $\hat{\tau}(x, s)$ via a standard causal machine learning method, such as a causal forest [Athey et al., 2019] or an X -learner [Künzel et al., 2019].
2. Choose state-specific treatment threshold c_s by maximizing an off-policy value estimate [e.g., Kallus and Uehara, 2022, Liao et al., 2022].

This is algorithmically much simpler than generic reinforcement learning, since we only need to consider problem dynamics when choosing the finite-dimensional threshold vector $c \in \mathbb{R}^{|\mathcal{S}|}$ in the second step—and can ignore dynamics when learning the potentially complex

³While the CADE $\tau(x, s)$ still needs to be estimated to construct the policy, it is independent of the policy π and can thus be directly estimated from offline data.

Algorithm 1 System-Aware State-Specific Targeting

- 1: **Data:** (X_i, S_i, W_i, Y_i) , $i = 1, \dots, n$
 - 2: **Require:** Grid $\mathbf{G} = \{(g_s)_{s \in \mathcal{S}} : g_s = b_i/B, b_i = 1, \dots, B-1, \forall s\}$
 - 3: Split the data into a training set and an evaluation set
 - 4: On the training set, train a causal machine learning model $\hat{\tau}$
 - 5: **for** $g \in \mathbf{G}$ **do**
 - 6: Set the threshold $c_s(g)$ to be the $(1 - g_s)$ th quantile of the estimates $\hat{\tau}(X_i, s)$ for all X_i in the training set, $\forall s$
 - 7: Obtain targeting rule $\pi_{i, \hat{\tau}, g} = I(\hat{\tau}(X_i, S_i) > c_{S_i}(g))$ for all units in the evaluation set
 - 8: On the evaluation set, estimate the policy value $\hat{\mu}(\pi_{\hat{\tau}, g})$ using an off-policy evaluation estimator.
 - 9: **end for**
 - 10: **Output:** Policy $\hat{\pi} = \operatorname{argmax}_{\pi_{\hat{\tau}, g}} \hat{\mu}(\pi_{\hat{\tau}, g})$
-

and high-dimensional function $\tau(x, s)$ in the first step. We now flesh out this approach and provide formal consistency result in the setting where the CADE $\tau(X, s)$ has a continuous distribution for all s . Our consistency results are achieved under reasonable choices for direct effect estimation and off-policy evaluation methods. In Section 3, we demonstrate how this algorithm can be applied to identify the optimal policy in a queuing system.

Our approach to targeting in dynamic systems is outlined in Algorithm 1. This algorithm leverages a causal machine learning algorithm to train a model for predicting CATE, which in our setting corresponds to the direct effect, $\tau(x, s)$. Building on a trained causal machine learning model, the algorithm searches over a grid on $(0, 1)^{|\mathcal{S}|}$, where each point on the grid corresponds to a targeting policy. For each point g on the grid, the corresponding policy treats everyone with an estimated CATE greater than a threshold, which is set as the $(1 - g_s)$ th quantile of the CATE estimates. The average outcomes of the policies are then computed using an off-policy evaluation estimator $\hat{\mu}(\pi)$, and the policy with the highest estimated outcome is selected.

Running Algorithm 1 requires splitting the sample into a training and evaluation set. This sample-splitting step may initially appear to be less straightforward, as the data points are correlated due to the system’s dynamics. However, for each fixed state $s \in \mathcal{S}$, the system regenerates whenever it returns to state s , and the data becomes independent of the preceding trajectory after each regeneration [Ross, 2014]. Therefore, we can split the dataset by first dividing the trajectory into i.i.d. chunks based on occurrences of a chosen state s , and then randomly assigning these chunks to the training or evaluation set. In practice, selecting a frequently visited state s as the splitting point may help ensure a more balanced split.

To explicitly indicate the dependency of the policy on the CADE function τ and the treatment proportion g , we sometimes write

$$\pi_{\tau, g}(x, s) = I(\tau(x, s) > \kappa_{1-g_s}(\tau(X_i, s))), \quad (9)$$

where $\kappa_m(\tau(X_i, s))$ is the m th quantile of the random variable $\tau(X_i, s)$. In other words, at each state, this policy assigns treatment to patients with $\tau(\cdot, s)$ in the top g -fraction. The optimal treatment proportion g^* and the threshold c^* associated with the optimal policy π^* satisfy the following conditions:

$$g_s^* \in \operatorname{argmax}_g \mu(\pi_{\tau, g}), \quad c_s^* = \kappa_{1-g_s^*}(\tau(X_i, s)), \quad \forall s \in \mathcal{S}, \quad (10)$$

and thus $\pi^* = \pi_{\tau, g^*}$.

2.3 Regret Bounds

We next provide some generic upper bounds—under abstract high-level conditions—on the regret attained by our proposed procedure. We will give more specific bounds in the context of queuing systems in the following section. Throughout, we will assume that—for every state s —the CADE $\tau(X_i, s)$ is continuously distributed with a density bounded away from both zero and infinity. This condition guarantees that the decision boundary $\tau(X_i, s) = c_s$ has sufficient spread around it, and that the quantile function $\kappa_m(\tau(X_i, s))$ is Lipschitz continuous in m .

Assumption 3 (Bounded Density of CADE). For all $s \in \mathcal{S}$, $\tau(X_i, s)$ has a density with respect to the Lebesgue measure that is bounded from above and below on its support.

Furthermore, we impose the following Lipschitz continuity assumption to ensure the smoothness of the density of the stationary distribution. This condition is typically satisfied when the Markov process induced by the policy π exhibits a nontrivial spectral gap [Cho and Meyer, 2001].

Assumption 4 (Lipschitz Continuity). There exist positive real constants L_d such that

$$|d_\pi(s) - d_{\pi'}(s)| \leq L_d \|\mathbb{E}[\pi(X_i, s)] - \mathbb{E}[\pi'(X_i, s)]\|_\infty, \quad \forall s \in \mathcal{S}. \quad (11)$$

For simplicity, we also make the following assumption that the optimal treatment proportion g^* is unique and well-separated.

Assumption 5 (Separation). For every $\epsilon > 0$,

$$\sup_{g: \|g^* - g\|_\infty \geq \epsilon} \mu(\pi_{\tau, g}) < \mu(\pi_{\tau, g^*}). \quad (12)$$

Theorem 3. Under Assumptions 1-5 and in the setting of Algorithm 1, assume further that $\hat{\tau}(X, s)$ is also continuously distributed for all s . Then, given access to an estimate $\hat{\tau}(x, s)$ learned on a held-out training set for which

$$\max_{s \in \mathcal{S}} \|\hat{\tau}(X_i, s) - \tau(X_i, s)\|_{L_2(P_X)} = \mathcal{O}_p(n^{-\beta}), \quad \beta > 0, \quad (13)$$

and an off-policy estimator that achieves

$$\sup_g |\hat{\mu}(\pi_{\hat{\tau}, g}) - \mu(\pi_{\tau, g})| = \mathcal{O}_p(n^{-\gamma}), \quad \gamma > 0, \quad (14)$$

and assuming that the grid resolution $B \rightarrow \infty$ fast enough such that

$$\hat{\mu}(\pi_{\hat{\tau}, \hat{g}}) \geq \sup_g \hat{\mu}(\pi_{\hat{\tau}, g}) - \mathcal{O}_p\left(n^{-\frac{2}{3}\beta} + n^{-\gamma}\right), \quad (15)$$

as $n \rightarrow \infty$, the policy $\hat{\pi}$ generated by Algorithm 1 satisfies

$$|\mu(\hat{\pi}) - \mu(\pi^*)| = \mathcal{O}_p\left(n^{-\frac{2}{3}\beta} + n^{-\gamma}\right). \quad (16)$$

The achieved error rate in (16) arises from two sources: an $\mathcal{O}_p(n^{-2\beta/3})$ error due to CATE estimation, and an $\mathcal{O}_p(n^{-2\beta/3} + n^{-\gamma})$ error from identifying the thresholds via M-estimation combined with off-policy evaluation. Specifically, for the latter one, the first term $\mathcal{O}_p(n^{-2\beta/3})$ reflects the use of the estimated CATE in off-policy evaluation, while the second term $\mathcal{O}_p(n^{-\gamma})$ captures the error from approximating the true value through off-policy evaluation. The overall convergence rate in (16) thus depends on both the direct effect estimation rate in (13) (measured in terms of the worst L_2 -error conditional on any state s), and the uniform convergence rate of the off-policy evaluation in (14). Under sufficient conditions, conventional off-policy evaluation methods, such as doubly robust approaches that combine the Q-estimation and importance weighting [Kallus and Uehara, 2022, Liao et al., 2022, Mehrabi and Wager, 2024], could often provide such guarantees in Markovian systems. In Section 3, we provide an example of a doubly robust that achieves a root- n uniform convergence rate for off-policy evaluation in the queuing context.

In Theorem 3, we require (13), a bound on the uniform $L_2(P_X)$ -norm of the estimated CATE function $\hat{\tau}(X_i, s)$ over states $s \in \mathcal{S}$. This condition is often attainable when the state space \mathcal{S} is finite, as assumed in Assumption 2, and a large body of literature has studied the L_2 -norm convergence rates achieved by nonparametric methods for estimating CATE (see, e.g., Kennedy [2023] for a discussion).⁴ When the CATE function is Hölder-smooth, stronger bounds on the sup-norm of the estimated CATE can often be achieved, which allows the error bound in (16) to be further tightened as follows.

Proposition 4. *Under Assumptions of Theorem 3, if instead of conditions (13) and (15), there exists $\beta > 0$ such that*

$$\sup_{s \in \mathcal{S}, x \in \mathcal{X}} \|\hat{\tau}(x, s) - \tau(x, s)\| = \mathcal{O}_p(n^{-\beta}), \quad (17)$$

and that the grid resolution $B \rightarrow \infty$ fast enough such that

$$\hat{\mu}(\pi_{\hat{\tau}, \hat{g}}) \geq \sup_g \hat{\mu}(\pi_{\hat{\tau}, g}) - \mathcal{O}_p(n^{-\beta} + n^{-\gamma}), \quad (18)$$

as $n \rightarrow \infty$, the policy $\hat{\pi}$ generated by Algorithm 1 satisfies

$$|\mu(\hat{\pi}) - \mu(\pi^*)| = \mathcal{O}_p(n^{-\beta} + n^{-\gamma}). \quad (19)$$

Remark 2. Algorithm 1 assumes that the direct effect $\tau(X, s)$ is continuous for all s and focuses on policies in the form of (8). This is often the case when the covariate is continuous, and the corresponding estimated CATE $\hat{\tau}(X, s)$ would also be continuous if machine learning methods such as causal forest are used to estimate CATE. However, Algorithm 1 can also be adjusted to accommodate cases where the covariate is discrete. In such cases, each grid point corresponds to a policy of the form (7), which requires specifying the parameters (c_s, p_s) . This motivates the following procedure of setting a grid for (c_s, p_s) : For a grid point g_s , if the distribution function of $\hat{\tau}(X_i, s)$ is continuous at the $(1 - g_s)$ th quantile, the algorithm sets $c_s(g)$ to the corresponding quantile and $p_s(g) = 0$. If, instead, the distribution function has a jump from q_1 to q_2 at the $(1 - g_s)$ th quantile, the algorithm sets $(c_s(g), p_s(g)) = (\kappa_{1-g_s}(\hat{\tau}(X_i, s)), (g_s - q_1)/(q_2 - q_1))$.

⁴One potential concern is that the units in our setting are correlated, and thus theories developed for CATE estimation in i.i.d. settings may not directly apply. However, we note that it is possible to construct a subset of the data with size $\mathcal{O}_p(n)$ by randomly selecting a single data point from each i.i.d. chunk, formed based on occurrences of some fixed chosen state s . This approach allows us to retain i.i.d.-like properties, so we still expect the same convergence rate to hold.

3 Application: Optimal Targeting in Queuing Systems

In this section, we show how to instantiate the abstract approach outlined in Section 2 in the context of queuing systems, and show how Theorem 3 yields a $1/\sqrt{n}$ -rate regret bound in this setting. We begin with the basic setting where data are collected from an $M/M/1$ queue with a maximum capacity of \bar{k} ,⁵ and the policy determines which units are admitted into the queue. In Sections 3.2 and 3.3, we extend the results to more complex queuing systems with parallel queues where the policy determines which units are routed to a faster service track, as well as settings where arrival rates are state-dependent and the objective is to maximize the total benefit over a fixed time horizon.

3.1 Targeting in a Simple Queueing Model

In an $M/M/1$ queue, patients arrive at a constant rate λ and are served at a constant rate μ , where both rates are bounded and bounded away from zero. We observe a sequence of n patient arrivals, indexed by $i = 1, \dots, n$, under a status quo behavior policy π_0 , which could be potentially unobserved. When a patient arrives, we observe their condition $X_i \in \mathcal{X}$, the current queue length $K_i = 1, \dots, \bar{k}$, assign a treatment $W_i \sim \pi(X_i, K_i)$ regarding whether to put them in the queue, and record their outcome Y_i . As in Assumption 2, we assume that the outcome Y_i is bounded almost surely. It is straightforward to verify that in such an $M/M/1$ queue, Assumptions 1 and 2 are satisfied when we regard the queue length K_i as the state.⁶

To use Algorithm 1, we need to find an off-policy evaluation estimator with an uniform guarantee. As we demonstrate, for the queuing setting under consideration, a doubly robust estimator achieves a root- n uniform consistency rate. For convenience, in the remainder of this section, we abuse the notation and sometimes let $\pi_w(x, s)$ denote the probability of assigning treatment w with covariate x and state s (i.e., $\pi_1(x, s) = \pi(x, s)$ and $\pi_0(x, s) = 1 - \pi(x, s)$). The underlying idea of this estimator arises from the observation that the expected outcome $\mu(\pi)$ can be decomposed as

$$\mu(\pi) = \sum_k \mathbb{E}_\pi [Y_i \mid K_i = k] \cdot d_\pi(k), \quad (20)$$

where the expectation is taken over the conditional distribution of Y_i given $K_i = k$ under π . This decomposition motivates an estimator of $\mu(\pi)$ by plugging in estimators for the conditional outcome $r_\pi(k) := \mathbb{E}_\pi [Y_i \mid K_i = k]$ and stationary density $d_\pi(k)$, both of which can be readily estimated in our setup.

The key insight for the estimation of $r_\pi(k)$ is that outcomes become independent after conditioning on the state K_i . Moreover, since there are only a finite number of possible states and $r_\pi(k)$ does not depend on the potentially high-dimensional covariate X_i , a simple sample average would suffice if (X_i, W_i) is drawn from the conditional distribution induced by the target policy π . Although the data is observed under π_0 , it is possible to employ the

⁵Alternatively, the system can be viewed as a queue without capacity constraints under a policy that assigns patients to control whenever the queue length reaches \bar{k} .

⁶Although Y_i , the outcome of patient i , may depend on the realized waiting time, when the patients are served at a constant rate μ that is independent of the state, the distribution of the realized waiting time is fully determined by the queue length at the time patient i joins the queue, and thus it still satisfies Assumption 1.

following doubly robust estimator for estimating the state-level value $r_\pi(k)$:

$$\hat{r}_\pi(k) := \sum_{i=1}^n I(K_i = k) \cdot \left[\hat{\eta}_\pi(X_i, k) + \frac{\pi_{W_i}(X_i, k)}{\hat{\pi}_{0,W_i}(X_i, k)} \cdot (Y_i - \hat{\eta}(W_i, X_i, k)) \right] \Big/ \sum_{i=1}^n I(K_i = k).$$

where $\hat{\eta}_\pi(X_i, k) = \mathbb{E}_\pi[\hat{\eta}(W_i, X_i, k) \mid X_i]$, and $\hat{\pi}_{0,W_i}(X_i, k)$ and $\hat{\eta}(W_i, X_i, k)$ are machine learning estimates of $\pi_{0,W_i}(X_i, k)$ and $\eta(W_i, X_i, k) := \mathbb{E}[Y_i \mid W_i, X_i, K_i = k]$, respectively.

To estimate the stationary density function $d_\pi(k)$, we leverage the fact that, in an $M/M/1$ queue, the system's transition rule and its stationary distribution can be explicitly expressed as functions of $\bar{\pi}$ and the unknown parameters λ and μ . Therefore, we approximate $d_\pi(k)$ by plugging in estimates of λ and μ , which can often be estimated well in a Poisson process setting like ours. In Section A of the supplementary material, we provide closed-form expressions for the corresponding stationary distribution d_π as functions of λ , μ , and $\bar{\pi}$.

Below, we show that the plug-in estimator

$$\hat{\mu}(\pi) = \sum_{k=0}^{\bar{k}} \hat{r}_\pi(k) \cdot \hat{d}_\pi(k) \quad (21)$$

achieves a \sqrt{n} uniform convergence rate, provided that there is sufficient overlap between the target policy π and the logging policy π_0 , and that the arrival and service rates are estimated at a parametric rate. As is standard in the literature on doubly robust methods [Kennedy, 2023, Kallus and Uehara, 2020], we assume that the machine learning estimates $\hat{\pi}_{0,w}(x, k)$ and $\hat{\eta}(w, x, k)$ are obtained using a separate sample or via cross-fitting, and that they are sufficiently accurate.

Assumption 6. For all treatments $w \in \{0, 1\}$ and states $k \in \{0, \dots, \bar{k}\}$, the nuisance estimates $\hat{\pi}_{0,w}(X_i, k)$ and $\hat{\eta}(w, X_i, k)$ the following product rate condition:

$$\|\hat{\pi}_{0,w}(X_i, k) - \pi_{0,w}(X_i, k)\|_{L_2(P_X)} \cdot \|\hat{\eta}(w, X_i, k) - \eta(w, X_i, k)\|_{L_2(P_X)} = \mathcal{O}_p\left(\frac{1}{\sqrt{n}}\right). \quad (22)$$

Moreover, $\hat{\pi}_{0,w}(x, k)$ and $\hat{\eta}(w, x, k)$ are estimated on a separate sample, and there exists universal constant $\Gamma_1 > 0$ and $\Gamma_2 < \infty$ such that $\hat{\pi}_{0,w}(x, k) \geq \Gamma_1$ and $\hat{\eta}(w, x, k) \leq \Gamma_2$ almost surely for all (w, s, k) .

Lemma 5. Under an $M/M/1$ queuing model as described, assume in addition that there the status-quo policy π_0 satisfies $\pi_{0,w}(x, k) > 0$ for all $x \in \mathcal{X}, k \in \{0, \dots, \bar{k}\}$, that the arrival and service rate estimators satisfy $\max(|\hat{\lambda} - \lambda|, |\hat{\mu} - \mu|) = \mathcal{O}_p(1/\sqrt{n})$, and that Assumption 6 holds. Then, for any fixed function $\tau : \mathcal{X} \times \{0, \dots, \bar{k}\} \rightarrow \mathbb{R}$ such that $\tau(X_i, k)$ is continuous for all k , the off-policy estimator $\hat{\mu}(\pi)$ achieves the following uniform rate of convergence:

$$\sup_{g \in (0,1)^{(\bar{k}+1)}} |\hat{\mu}(\pi_{\tau,g}) - \bar{\mu}(\pi_{\tau,g})| = \mathcal{O}_p\left(n^{-1/2}\right). \quad (23)$$

Plugging the result from Lemma 5 into Theorem 3 and Proposition 4 suggests that the convergence rate of our targeting algorithm is always dominated by the CATE estimation error, which matches the rate of the direct targeting rule that ignores the state dynamics.

This suggests that incorporating the system state yields policies that are asymptotically no worse, and often better, than those that ignore dynamics, without incurring additional convergence penalties. Moreover, when the CATE function is Hölder-smooth and the estimator $\hat{\tau}$ achieves the rate in (17) with $\beta = 1/2$, the value of the learned policy from Algorithm 4 converges to the optimal policy value at a parametric rate.

Corollary 6. *Under the conditions of Lemma 5 and given a CADE estimator satisfying (13), our learned policy has regret on the order of $\mu(\pi^*) - \mu(\hat{\pi}) = \mathcal{O}_P(n^{-2\beta/3})$.*

When the maximum queue length \bar{k} is large, modeling the thresholds c_k (or equivalently, the treatment proportions g_k) as functions of k can sometimes lead to improved finite-sample performance. This parallels common practice in policy learning for MDPs, where treatment probabilities $\pi(x, k)$ are often modeled as functions of both x and k [Sutton and Barto, 2018]. As in those settings, parametrization introduces additional approximation error depending on how well the chosen functional form captures the true thresholds. However, since our policy space is much simpler than that of general MDPs, the quality of approximation is often better in practice.

Remark 3. We allow the status-quo policy to be potentially unobserved. When it is known exactly, a simple importance weighting estimator would suffice for off-policy evaluation. In our setup, we make the implicit assumption that the status-quo policy depends only on (X_i, K_i) , the information available at individual i 's arrival, and not on other aspects of the history or future. This assumption, often referred to as sequential ignorability [Hernán and Robins, 2020], is reasonable in our context, as individuals are typically routed based solely on features observable to the system at the time of arrival.

3.2 Optimal Routing with Parallel Queues

In the basic setting considered above, the policy determines whether to admit an individual into a single queue. In many practical systems, however, individuals can be routed to parallel queues with different service speeds, and the decision lies in routing each arriving individual to one of the available service tracks. For example, in emergency departments, triage nurses need to decide whether to route a patient to a fast-track urgent care line or a regular treatment line; similarly, in online delivery platforms, the system need to decide whether to assign a customer to expedited delivery or assign them to standard delivery.

We show how our framework can be extended to accommodate such parallel queuing systems by augmenting the state space, where routing decisions influence not only individual outcomes but also system dynamics in both of the queues. In such a parallel queuing system, individuals arrive according to a Poisson process with rate λ and are routed to one of two queues, where each queue $j \in \{0, 1\}$ has its own service rate μ_j and maximum capacity \bar{k}_j . The two queues operate independently, and service proceeds only if the respective queue is non-empty.

Upon each arrival, we observe the individual's covariate X_i as well as the current queue lengths (K_{0i}, K_{1i}) , and assign a treatment $W_i \sim \pi(X_i, K_{0i}, K_{1i})$ indicating whether the individual is routed to queue 0 or 1. When one of the queues is full and the other is not, the arriving individual is always routed to the non-full queue regardless of the treatment, and there will be no arrivals when both of the queues are full. After assignment, we record the outcome Y_i , which could depend on the individual's covariates and the realized wait and service times in the assigned queue. As before, we assume Y_i is bounded almost surely.

To verify that our framework could be extended to this setting, we note that this is a discrete-time Poisson point process observed at arrivals. Under a fixed routing policy $W_i \sim \pi$, the evolution of the queue lengths (K_{0i}, K_{1i}) follows a time-homogeneous Markov decision process such that

$$\begin{aligned} K_{0,i+1} &= K_{0i} + 1 - W_i \cdot I(K_{1i} = \bar{k}_1) - N_{\text{served},i}, \\ K_{1,i+1} &= K_{1i} + 1 - (1 - W_i) \cdot I(K_{0i} = \bar{k}_1) - N_{\text{served},i}, \end{aligned} \quad (24)$$

where $N_{\text{served},i}$ denotes the total number of individuals served between the i th and the $i + 1$ th arrivals. We refer readers to Section A of the supplementary material for details on the state dynamics of this system.

Since arrivals and services follow Poisson processes, this embedded process recorded at arrivals satisfy Assumptions 1-2. We can thus extend our off-policy evaluation and learning guarantees to these more complex systems, where now we need to search for $(\bar{k}_0 + 1) \times (\bar{k}_1 + 1)$ thresholds. In Section 4.2, we show in simulation study that the extended algorithm learns a system-aware targeting policy that always outperforms the direct targeting benchmark and converges toward the optimal policy as the sample size increases.

Remark 4. By augmenting the state space, our framework can also accommodate dynamic resource allocation problems. Upon each arrival, the system observes both the current resource level and the covariates of the incoming individual including their resource demand, and must decide whether to approve the request. This setup fits naturally into our framework by defining the state as the pair of the current resource level and the individual's demand. This formulation also captures scenarios with multiple types of operations that require different service times (e.g., major versus minor medical procedures, long-distance versus short-distance deliveries), where each type corresponds to a different resource demand level of the service.

3.3 Optimizing Long-Run Reward Rate with State-Dependent Arrivals

In the baseline setup, we assumed that arrivals follow a Poisson process with a constant rate λ . However, in many real-world systems, the arrival rate may vary with the current congestion level. For example, users may choose to leave or avoid a digital platform if they anticipate long waiting times. In such settings, the routing policy influences not only the outcomes experienced by individuals who enter the system, but also the total number of arrivals. Consequently, the objective may shift from maximizing the average outcome per user to optimizing the overall benefit accumulated over a fixed time period, such as daily revenue.

To accommodate this setting, we extend our framework to model data collected from an $M_n/M/1$ queue. Throughout, we observe a sequence of events $\{\mathbf{E}_i\}_{i=1,\dots,N(T)}$ occurring at time $0 < T_1 < T_2 < \dots < T_{N(T)} < T$, where $N(t) = \max\{i : T_i \leq t\}$ counts the total number of events up to time t . Each event represents either an individual arriving ($A_i = 1$) or leaving ($A_i = 0$) the system. If an individual arrives (i.e., $A_i = 1$), we observe their condition $X_i \in \mathcal{X}$, the current queue length $K_i = 1, \dots, \bar{k}$, assign a treatment $W_i \sim \pi(X_i, K_i)$ regarding whether to put them in the queue, and record their outcome R_i . If the event represents an individual leaving the system, we define $X_i = \emptyset$, $W_i = 2$, and $R_i = 0$ as placeholders.

In an $M_n/M/1$ queue, patients arrive at a rate of λ_k and are served at a rate of μ , where k represents the queue length at the time of the patient's arrival. Each time a patient arrives or leaves the system, the queue length may change, which can, in turn, affect the arrival of future events and the outcomes experienced by other patients remaining in the queue. To account for this, we denote the interarrival time of events as $\Delta_i := T_i - T_{i-1}$, which may be correlated with the queue length K_i .

To summarize, we write $\mathbf{E}_i = (X_i, K_i, A_i, W_i, \Delta_i, R_i)$, where X_i is the incoming patient's condition, A_i is the event type, K_i is the queue length at time T_i , Δ_i is the interarrival time between this event and the previous event, W_i is the treatment assigned to the incoming patient, and R_i is the patient's reward. Specifically, if we define $S_i = (K_i, A_i)$ and $Y_i = (R_i, \Delta_i)$, this recovers the model we introduced in Section 2.

In Section 2, we defined the optimal policy as the treatment assignment rule that maximizes the average reward, $\mu(\pi)$. However, depending on the context, one may sometimes be more interested in maximizing the long-run reward rate, which can be defined as

$$\theta(\pi) = \mathbb{E}_\pi \left[\lim_{T \rightarrow \infty} \frac{1}{T} \sum_{i=1}^{N(T)} R_i \right]. \quad (25)$$

In other words, $\theta(\pi)$ measures the average reward the system achieves per unit of time in the long run. In an $M/M/1$ queuing system where the patient's arrival rate is constant, maximizing $\theta(\pi)$ is equivalent to maximizing $\mu(\pi)$. However, when the patient's arrival rate varies across the queue length, the two objectives become subtly different. For example, if the treatment is in terms of health administration, one would optimize $\mu(\pi)$ if the goal is to improve health outcomes on average for every patient that arrives at the hospital. On the other hand, one would optimize $\theta(\pi)$ if the goal is to maximize the total benefit (e.g., the overall amount of health improvement) obtained within a fixed amount of time. Nevertheless, as we show below, the form of the optimal policy remains the same as the one derived in Theorem 2, even when the objective is to optimize the long-run reward rate.

Corollary 7. *Under an $M_n/M/1$ queuing model as described, there exists a policy π^* that*

$$\pi^*(x, s) \in \arg \max_{\pi} \theta(\pi). \quad (26)$$

and admits the form

$$\pi^*(x, s) = I(\tau(x, s) > c_s) + I(\tau(x, s) = c_s) \cdot p_s \quad (27)$$

for some constant $c_s \in \mathbb{R}$ and $p_s \in [0, 1]$, $\forall x \in \mathcal{X}, s \in \mathcal{S}$. Furthermore, if the direct effect $\tau(X, s)$ is continuous for all s , π^ reduces to the form*

$$\pi^*(x, s) = I(\tau(x, s) > c_s). \quad (28)$$

To search for the optimal policy π^* , we need to evaluate the long-run reward rate $\theta(\pi)$ for all policies π of the form given in Corollary 7, using data collected under the status quo policy π_0 . A useful observation is that the long-run reward rate can be expressed as the ratio of two average outcomes, which is a standard result in the Markov renewal process literature (see, e.g., Chapter 7 of Ross [2014]).

Lemma 8 (Renewal Reward Theorem). *Under an $M_n/M/1$ queuing model as described,*

$$\theta(\pi) = \frac{\mathbb{E}_\pi[R_i]}{\mathbb{E}_\pi[\Delta_i]}, \quad (29)$$

where the expectations are taken over d_π , the stationary distribution of the associated point process induced by policy π , with

$$d_\pi(s) = \lim_{t \rightarrow \infty} \frac{\sum_{i=1}^{N(t)} \mathbb{P}_\pi[S_i = s]}{N(t)}. \quad (30)$$

This representation allows us to estimate the reward rate θ_π by separately estimating $\mathbb{E}_\pi[R_i]$ and $\mathbb{E}_\pi[\Delta_i]$, for which we can directly apply the doubly robust estimator developed in Lemma 5. One may then appeal to the uniform delta method [van der Vaart, 1998] to argue that the resulting plug-in estimator of the reward rate should follow the same asymptotic guarantee as $\hat{\mu}$ in Lemma 5.

4 Numerical Examples

In this section, we evaluate the performance of Algorithm 1, our proposed state-specific targeting rule, and compare it to the benchmark direct targeting rule using synthetic data generated from queuing dynamics. We revisit the settings from Sections 3.2 and 3.3, and assess how different targeting strategies influence the steady-state distribution and long-run outcomes.

4.1 Targeting with Congestion-Sensitive Arrivals

To start with, we consider an $M_n/M/1$ queue as introduced in Section 3.3, and study its behavior under different policies. For each user i arriving at the system, we generate their covariates from a 10-dimensional normal distribution, $X_i \sim N(0, I_{10})$, where I_{10} is the 10×10 identity matrix. For the queuing dynamics, the users' arrival rate is set to be

$$\lambda_k = \begin{cases} 2/(k+1)^{0.1}, & k = 0, \dots, 19, \\ 0, & k = 20, \end{cases} \quad (31)$$

and the service rate is set to be

$$\mu_k = \begin{cases} 0, & k = 0, \\ 1, & k = 1, \dots, 20. \end{cases} \quad (32)$$

We consider a logging policy π_0 that assigns user i to the queue with a probability of $\pi_0(X_i, K_i)$, where

$$\pi_0(x, k) = 0.6 + 0.2I(x_2 > 0) - 0.1I(x_4 + x_5 > 0), \quad (33)$$

which is unknown to the policy maker. The user's outcome Y_i is then generated as

$$Y_i = W_i \cdot \{(7 - K_i)|X_{i,1}| + 3X_{i,2}\} + \max\{X_{i,3}, 0\} + \epsilon_i, \quad \epsilon_i \sim N(0, 4). \quad (34)$$

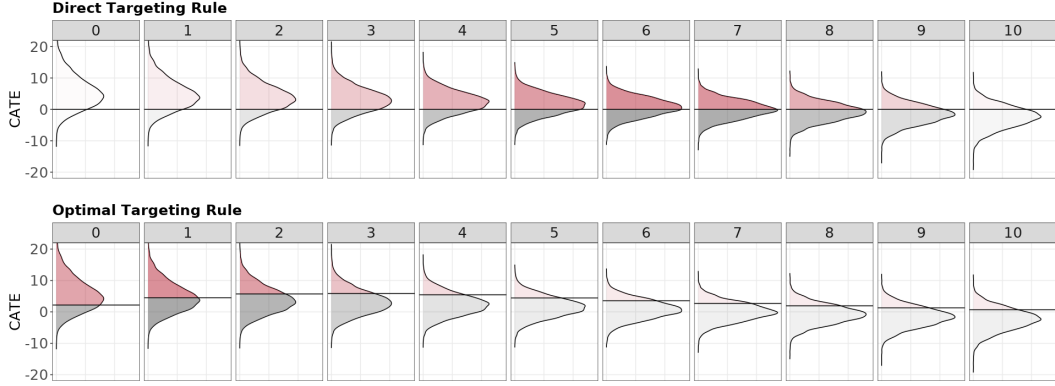


Figure 2: Targeting rules for users arriving at the system with different queue lengths ($k = 0, \dots, 10$). The curves in each panel show the distribution of $\tau(X_i, k)$ for users arriving when the queue length is k . The horizontal line represents the treatment threshold c_k , which is fixed at zero under the direct targeting rule. The red area shows users who are assigned treatment (with CATE values above the threshold), while the grey area shows users who are not treated (with CATE values below the threshold). The intensity of the colors represents how often users experience each queue length, with darker colors indicating more frequent occurrences.

In particular, users with a larger $X_{i,1}$ are more sensitive to the change in queue length—they benefit more from getting a timely treatment, but also suffer more from the delay in receiving the treatment.

To approximate the optimal policy, we search over the policy class composed of policies of the form (28), satisfying the constraint that $\mathbb{P}[\pi(X_i, k_1)] \geq \mathbb{P}[\pi(X_i, k_2)]$ if $k_1 \geq k_2$. To do so, we use the “NLOPT.LN.COBYLA” function in the R package “nloptr” [Johnson, 2008], which implements a C-based COBYLA (Constrained Optimization BY Linear Approximations) algorithm for derivative-free optimization with nonlinear inequality and equality constraints [Powell, 1994, 1998].

A comparison between the approximated optimal policy and the direct policy is illustrated in Figure 2. In general, we observe that the optimal policy is more stringent (or parsimonious) in selecting users into the queue. This is particularly true when the queue length is smaller, where a large portion of the users have a positive treatment effect. This result may seem counterintuitive—typically, one would expect that when the queue length is shorter, more users could be accommodated. However, as shown in Figure 2, this more selective targeting strategy significantly reduces the average waiting time, resulting in most users arriving when the queue length is less than 5. By withholding treatment from a smaller fraction of users with lower CATE, the policy ensures that when users with more urgent conditions arrive, their needs can be met timely.

Next, we examine the policy generated by Algorithm 1 using a dataset observed over a time period of length T and compare its performance to the approximated optimal policy. We also consider a baseline algorithm that applies direct targeting using CATE obtained from a causal forest trained on the same dataset. The resulting policy consists of both a trained random forest and a set of thresholds. To evaluate the long-run reward rate under the learned policies, we compute the conditional CATE distribution with Monte Carlo

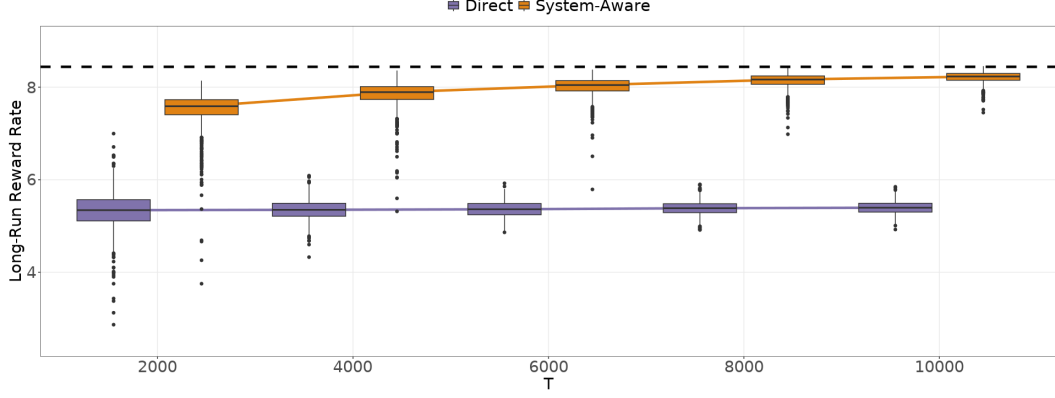


Figure 3: Long-run reward rates achieved by policies generated using Algorithm 1 and a causal forest with the direct targeting rule, respectively. The dashed vertical line represents the optimal long-run reward rate approximated using the ground truth with policy shown in Figure 2.

approximations and the stationary distribution analytically with the formulas provided in Section A of the supplementary material. We vary T from 2,000 to 10,000 and repeat the process 1,000 times for each horizon length considered.

Figure 3 illustrates the long-run reward rates achieved by the policies generated from Algorithm 1 and those derived from direct targeting using CATE estimates from a causal forest. As the time horizon T increases, the performance of the policies learned by Algorithm 1 improves, with the long-run reward rate steadily approaching the optimal reward rate indicated by the dashed line. In contrast, the reward rate achieved by the direct targeting approach remains consistently lower across all values of T . As T increases, we observe a reduction in the variance of the reward rates for both methods.

4.2 Routing with Parallel Queues

We also evaluate our proposed algorithm under the setting described in Section 3.2, where patients arrive sequentially and must be routed to one of two queues upon arrival. For each patient i , we observe covariates generated from a 10-dimensional standard normal distribution, $X_i \sim N(0, I_{10})$. The queue lengths for the regular and fast-track queues upon arrival are denoted by $K_{0i} \in \{0, 1, \dots, 10\}$ and $K_{1i} \in \{0, 1, 2, 3\}$, respectively. We set the arrival rate to $\lambda = 1$, and the service rates to $\mu_0 = 0.5$.

Upon patient i 's arrival, a treatment $W_i \in \{0, 1\}$ is assigned according to a random draw from a Bernoulli(0.5) distribution, where $W_i = 1$ indicates routing to the fast-track queue and $W_i = 0$ indicates routing to the regular queue. The outcome Y_i is generated as

$$Y_i = -\log(\text{waiting}_i + \text{service}_i) \cdot \mathbb{I}(X_{i,1} \leq Z_{0.75}) - 3(\text{waiting}_i + \text{service}_i)^2 \cdot \mathbb{I}(X_{i,1} > Z_{0.75}) + \epsilon_i,$$

where $\epsilon_i \sim N(0, 1)$ and $Z_{0.75}$ denotes the 75th percentile of the marginal distribution of $X_{i,1}$. In other words, 25% of patients are sensitive to treatment delays and would experience worse outcomes if waiting is prolonged.

We compare the performance of the proposed system-aware targeting rule with the benchmark direct targeting rule. To identify the optimal policy, we again employ the R

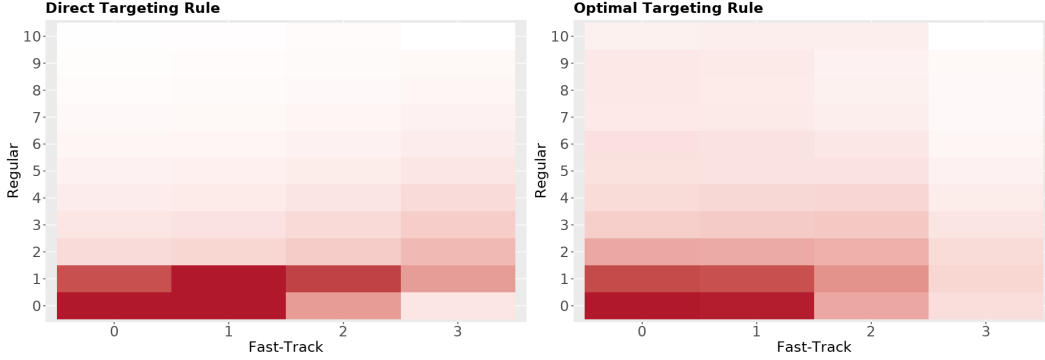


Figure 4: Stationary distribution of queue lengths (K_{1i}, K_{0i}) under the direct targeting rule and the optimal targeting rule, respectively. The intensity of the colors represents how often users experience each combination of queue lengths, with darker colors indicating more frequent occurrences.

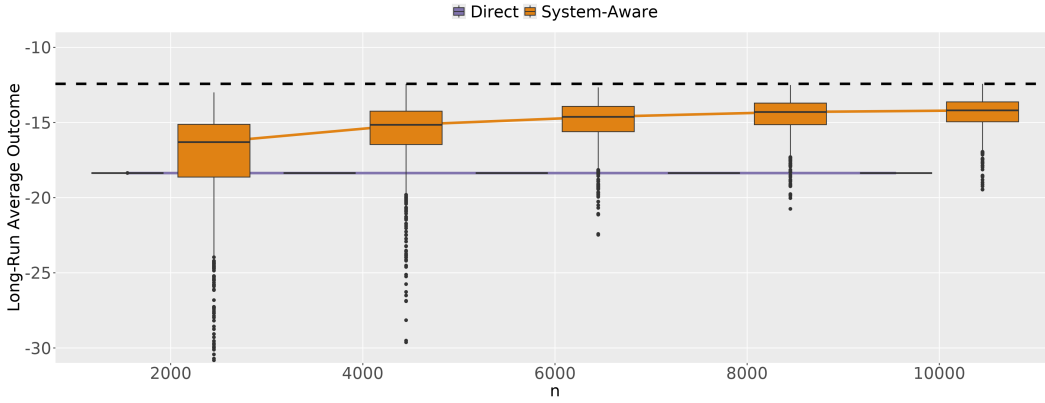


Figure 5: Long-run average outcomes achieved by policies generated using Algorithm 1 and a causal forest with the direct targeting rule, respectively. The dashed vertical line represents the optimal long-run average outcome approximated using the ground truth with policy shown in Figure 4.

function “NLOPT_LN_COBYLA”, with the long-run average outcome computed under the ground-truth data-generating process and the stationary distribution analytically derived from the transition matrix given in Section A of the supplementary material.

As shown in Figure 4, the optimal targeting rule shifts stationary density mass away from congested fast-track states such as $(3, k_0)$ toward less crowded states like (k_1, k_0) for $k_1 \in \{0, 1, 2\}$. This allows the system to preserve fast-track capacity so that, when patients with urgent conditions arrive, they can be admitted promptly. In contrast, the direct targeting rule tends to overutilize the fast-track queue, resulting in heavier congestion and a more imbalanced state distribution. Overall, the optimal targeting rule achieves a 16% improvement in the long-run average outcome.

We now evaluate Algorithm 1 in the parallel queue setting using the same simulation

setup and estimation procedure described in Section 4.1. Figure 5 summarizes the performance of the two policies across sample sizes $n = \{2000, \dots, 10000\}$. Notably, the direct targeting rule, based on CATE estimates from a causal forest, performs consistently poorly across all repetitions and sample sizes. In fact, the resulting policy always routes patients to the fast-track queue whenever it is not full, regardless of the patients’ covariates. In contrast, the system-aware policy learned through our proposed algorithm steadily improves with more data and converges toward the optimal policy as n increases.

Acknowledgment

This research was supported by the ONR under grant N000142412091.

References

- Shipra Agrawal and Randy Jia. Learning in structured mdps with convex cost functions: Improved regret bounds for inventory management. In *Proceedings of the 2019 ACM Conference on Economics and Computation*, pages 743–744, 2019.
- Peter M Aronow and Cyrus Samii. Estimating average causal effects under general interference, with application to a social network experiment. *The Annals of Applied Statistics*, 11(4):1912–1947, 2017.
- Susan Athey and Guido Imbens. Recursive partitioning for heterogeneous causal effects. *Proceedings of the National Academy of Sciences*, 113(27):7353–7360, 2016.
- Susan Athey and Stefan Wager. Policy learning with observational data. *Econometrica*, 89(1):133–161, 2021.
- Susan Athey, Julie Tibshirani, and Stefan Wager. Generalized random forests. *The Annals of Statistics*, 47(2):1148–1178, 2019.
- Gah-Yi Ban and Cynthia Rudin. The big data newsvendor: Practical insights from machine learning. *Operations Research*, 67(1):90–108, 2019.
- Guillaume W Basse, Avi Feller, and Panos Toulis. Randomization tests of causal effects under interference. *Biometrika*, 106(2):487–494, 2019.
- Dimitris Bertsimas and Nathan Kallus. From predictive to prescriptive analytics. *Management Science*, 66(3):1025–1044, 2020.
- Debopam Bhattacharya and Pascaline Dupas. Inferring welfare maximizing treatment assignment under budget constraints. *Journal of Econometrics*, 167(1):168–196, 2012.
- Christian Borgs, Jennifer T Chayes, Sherwin Doroudi, Mor Harchol-Balter, and Kuang Xu. The optimal admission threshold in observable queues with state dependent pricing. *Probability in the Engineering and Informational Sciences*, 28(1):101–119, 2014.
- Justin Boutilier, Jonas Oddur Jonasson, Hannah Li, and Erez Yoeli. Randomized controlled trials of service interventions: The impact of capacity constraints. *arXiv preprint arXiv:2407.21322*, 2024.

- Boxiao Chen, Jiashuo Jiang, Jiawei Zhang, and Zhengyuan Zhou. Learning to order for inventory systems with lost sales and uncertain supplies. *Management Science*, 70(12):8631–8646, 2024.
- Hong Chen and Murray Z Frank. State dependent pricing with a queue. *IIE Transactions*, 33(10):847–860, 2001.
- Xi Chen, Zachary Owen, Clark Pixton, and David Simchi-Levi. A statistical learning approach to personalization in revenue management. *Management Science*, 68(3):1923–1937, 2022.
- Victor Chernozhukov, Denis Chetverikov, Mert Demirer, Esther Duflo, Christian Hansen, Whitney Newey, and James Robins. Double/debiased machine learning for treatment and structural parameters, 2018.
- Victor Chernozhukov, Juan Carlos Escanciano, Hidehiko Ichimura, Whitney K Newey, and James M Robins. Locally robust semiparametric estimation. *Econometrica*, 90(4):1501–1535, 2022.
- Wang Chi Cheung and David Simchi-Levi. Sampling-based approximation schemes for capacitated stochastic inventory control models. *Mathematics of Operations Research*, 44(2):668–692, 2019.
- Grace E Cho and Carl D Meyer. Comparison of perturbation bounds for the stationary distribution of a markov chain. *Linear Algebra and its Applications*, 335(1-3):137–150, 2001.
- Thomas Dietterich, George Trimonias, and Zhitang Chen. Discovering and removing exogenous state variables and rewards for reinforcement learning. In *International Conference on Machine Learning*, pages 1262–1270. PMLR, 2018.
- Jingying Ding, Woonghee Tim Huh, and Ying Rong. Feature-based inventory control with censored demand. *Manufacturing & Service Operations Management*, 26(3):1157–1172, 2024.
- Yonathan Efroni, Dylan J Foster, Dipendra Misra, Akshay Krishnamurthy, and John Langford. Sample-efficient reinforcement learning in the presence of exogenous information. In *Conference on Learning Theory*, pages 5062–5127. PMLR, 2022.
- Vivek Farias, Andrew Li, Tianyi Peng, and Andrew Zheng. Markovian interference in experiments. *Advances in Neural Information Processing Systems*, 35:535–549, 2022.
- Max H Farrell, Tengyuan Liang, and Sanjog Misra. Deep neural networks for estimation and inference. *Econometrica*, 89(1):181–213, 2021.
- Qi Feng and J George Shanthikumar. How research in production and operations management may evolve in the era of big data. *Production and Operations Management*, 27(9):1670–1684, 2018.
- Andrea Galeotti, Benjamin Golub, and Sanjeev Goyal. Targeting interventions in networks. *Econometrica*, 88(6):2445–2471, 2020.

- Miguel A Hernán and James M Robins. *Causal Inference: What If*. Chapman & Hall/CRC, Boca Raton, 2020.
- Keisuke Hirano and Jack R Porter. Asymptotics for statistical treatment rules. *Econometrica*, 77(5):1683–1701, 2009.
- Ronald A Howard. *Dynamic Programming and Markov Processes*. John Wiley and Sons/MIT Press, 1960.
- Yuchen Hu, Shuangning Li, and Stefan Wager. Average direct and indirect causal effects under interference. *Biometrika*, 109(4):1165–1172, 2022.
- Xinyang Huang and Jin Xu. Estimating individualized treatment rules with risk constraint. *Biometrics*, 76(4):1310–1318, 2020.
- Michael G Hudgens and M Elizabeth Halloran. Toward causal inference with interference. *Journal of the American Statistical Association*, 103(482):832–842, 2008.
- Peter S Hussey, Jeanne S Ringel, Sangeeta Ahluwalia, Rebecca Anhang Price, Christine Buttorff, Thomas W Concannon, Susan L Lovejoy, Grant R Martsolf, Robert S Rudin, Dana Schultz, et al. Resources and capabilities of the department of veterans affairs to provide timely and accessible care to veterans. *Rand Health Quarterly*, 5(4), 2016.
- Kosuke Imai and Michael Lingzhi Li. Experimental evaluation of individualized treatment rules. *Journal of the American Statistical Association*, 118(541):242–256, 2023.
- Evin Uzun Jacobson, Nilay Tanık Argon, and Serhan Ziya. Priority assignment in emergency response. *Operations Research*, 60(4):813–832, 2012.
- Søren Glud Johansen and Shaler Stidham Jr. Control of arrivals to a stochastic input–output system. *Advances in Applied Probability*, 12(4):972–999, 1980.
- Ramesh Johari, Hannah Li, Anushka Murthy, and Gabriel Y Weintraub. When does interference matter? decision-making in platform experiments. *arXiv preprint arXiv:2410.06580*, 2024.
- Steven G. Johnson. *The NLOpt nonlinear-optimization package*, 2008. URL <https://github.com/stevengj/nlopt>.
- Nathan Kallus. Balanced policy evaluation and learning. *Advances in neural information processing systems*, 31, 2018.
- Nathan Kallus and Masatoshi Uehara. Double reinforcement learning for efficient off-policy evaluation in markov decision processes. *J. Mach. Learn. Res.*, 21:167–1, 2020.
- Nathan Kallus and Masatoshi Uehara. Efficiently breaking the curse of horizon in off-policy evaluation with double reinforcement learning. *Operations Research*, 70(6):3282–3302, 2022.
- Nathan Kallus and Angela Zhou. Minimax-optimal policy learning under unobserved confounding. *Management Science*, 67(5):2870–2890, 2021.
- Edward H Kennedy. Towards optimal doubly robust estimation of heterogeneous causal effects. *Electronic Journal of Statistics*, 17(2):3008–3049, 2023.

- N Bora Keskin and Can Zhang. Feature-based scheduling and dynamic learning with a large backlog. *Available at SSRN 4852356*, 2024.
- Toru Kitagawa and Aleksey Tetenov. Who should be treated? empirical welfare maximization methods for treatment choice. *Econometrica*, 86(2):591–616, 2018.
- Toru Kitagawa and Guanyi Wang. Individualized treatment allocation in sequential network games. *arXiv preprint arXiv:2302.05747*, 2023a.
- Toru Kitagawa and Guanyi Wang. Who should get vaccinated? individualized allocation of vaccines over sir network. *Journal of Econometrics*, 232(1):109–131, 2023b.
- Sören R Künzel, Jasjeet S Sekhon, Peter J Bickel, and Bin Yu. Metalearners for estimating heterogeneous treatment effects using machine learning. *Proceedings of the national academy of sciences*, 116(10):4156–4165, 2019.
- Hoang Le, Cameron Voloshin, and Yisong Yue. Batch policy learning under constraints. In *International Conference on Machine Learning*, pages 3703–3712. PMLR, 2019.
- Michael P Leung. Rate-optimal cluster-randomized designs for spatial interference. *The Annals of Statistics*, 50(5):3064–3087, 2022.
- Shuangning Li and Stefan Wager. Random graph asymptotics for treatment effect estimation under network interference. *arXiv preprint arXiv:2007.13302*, 2020.
- Shuangning Li, Ramesh Johari, Xu Kuang, and Stefan Wager. Experimenting under stochastic congestion. *arXiv preprint arXiv:2302.12093*, 2023.
- Peng Liao, Predrag Klasnja, and Susan Murphy. Off-policy estimation of long-term average outcomes with applications to mobile health. *Journal of the American Statistical Association*, 116(533):382–391, 2021.
- Peng Liao, Zhengling Qi, Runzhe Wan, Predrag Klasnja, and Susan A Murphy. Batch policy learning in average reward markov decision processes. *The Annals of Statistics*, 50(6):3364–3387, 2022.
- Alex Luedtke and Antoine Chambaz. Performance guarantees for policy learning. *Annales de l’IHP Probabilités et statistiques*, 56(3):2162, 2020.
- Alexander R Luedtke and Mark J van der Laan. Optimal individualized treatments in resource-limited settings. *The International Journal of Biostatistics*, 12(1):283–303, 2016.
- Charles F. Manski. Statistical treatment rules for heterogeneous populations. *Econometrica*, 72(4):1221–1246, 2004. doi: <https://doi.org/10.1111/j.1468-0262.2004.00530.x>.
- Charles F Manski. *Identification for prediction and decision*. Harvard University Press, 2009.
- Charles F Manski. Identification of treatment response with social interactions. *The Econometrics Journal*, 16(1):S1–S23, 2013.
- Andreas Maurer. A vector-contraction inequality for rademacher complexities. In *Algorithmic Learning Theory*, pages 3–17, Cham, 2016. Springer International Publishing.

- Mohammad Mehrabi and Stefan Wager. Off-policy evaluation in markov decision processes under weak distributional overlap. *arXiv preprint arXiv:2402.08201*, 2024.
- Harvey W Meislin, Sally A Coates, Janine Cyr, and Terry Valenzuela. Fast track: Urgent care within a teaching hospital emergency department: Can it work? *Annals of Emergency Medicine*, 17(5):453–456, 1988.
- Alex F Mills, Nilay Tanik Argon, and Serhan Ziya. Resource-based patient prioritization in mass-casualty incidents. *Manufacturing & Service Operations Management*, 15(3):361–377, 2013.
- Evan Munro, Xu Kuang, and Stefan Wager. Treatment effects in market equilibrium. *American Economic Review*, forthcoming, 2025.
- Susan A Murphy. Optimal dynamic treatment regimes. *Journal of the Royal Statistical Society: Series B (Statistical Methodology)*, 65(2):331–355, 2003.
- Susan A Murphy. A generalization error for q-learning. *Journal of Machine Learning Research*, 6:1073–1097, 2005.
- Karthikey Murthy, Divya Padmanabhan, and Satyanath Bhat. Admission control in the presence of arrival forecasts with blocking-based policy optimization. In *2022 Winter Simulation Conference (WSC)*, pages 2270–2281. IEEE, 2022.
- Pinhas Naor. The regulation of queue size by levying tolls. *Econometrica*, 37(1):15–24, 1969.
- Xinkun Nie and Stefan Wager. Quasi-oracle estimation of heterogeneous treatment effects. *Biometrika*, 108(2):299–319, 2021.
- Xinkun Nie, Emma Brunskill, and Stefan Wager. Learning when-to-treat policies. *Journal of the American Statistical Association*, 116(533):392–409, 2021.
- Michael JD Powell. *A Direct Search Optimization Method That Models the Objective and Constraint Functions by Linear Interpolation*, pages 51–67. Springer Netherlands, Dordrecht, 1994.
- Michael JD Powell. Direct search algorithms for optimization calculations. *Acta numerica*, 7:287–336, 1998.
- Min Qian and Susan A Murphy. Performance guarantees for individualized treatment rules. *Annals of Statistics*, 39(2):1180, 2011.
- James M Robins. Optimal structural nested models for optimal sequential decisions. In *Proceedings of the second seattle Symposium in Biostatistics*, pages 189–326. Springer, 2004.
- Sheldon Ross. *Introduction to Probability Models (Eleventh Edition)*. Academic Press, Boston, eleventh edition edition, 2014.
- Fredrik Sävje, Peter M Aronow, and Michael G Hudgens. Average treatment effects in the presence of unknown interference. *The Annals of Statistics*, 49(2):673–701, 2021.

- Yunting Shi, Nan Liu, and Guohua Wan. Treatment planning for victims with heterogeneous time sensitivities in mass casualty incidents. *Operations Research*, 72(4):1400–1420, 2024.
- Sean R Sinclair, Felipe Vieira Frujeri, Ching-An Cheng, Luke Marshall, Hugo De Oliveira Barbalho, Jingling Li, Jennifer Neville, Ishai Menache, and Adith Swaminathan. Hind-sight learning for mdps with exogenous inputs. In *International Conference on Machine Learning*, pages 31877–31914. PMLR, 2023.
- Jörg Stoye. Minimax regret treatment choice with finite samples. *Journal of Econometrics*, 151(1):70–81, 2009.
- Jörg Stoye. Minimax regret treatment choice with covariates or with limited validity of experiments. *Journal of Econometrics*, 166(1):138–156, 2012.
- Hao Sun, Evan Munro, Georgy Kalashnov, Shuyang Du, and Stefan Wager. Treatment allocation under uncertain costs. *arXiv preprint arXiv:2103.11066*, 2021.
- Liyang Sun. Empirical welfare maximization with constraints. *arXiv preprint arXiv:2103.15298*, 2, 2021.
- Richard S. Sutton and Andrew G. Barto. *Reinforcement Learning: An Introduction*. A Bradford Book, Cambridge, MA, USA, 2018. ISBN 0262039249.
- Richard S Sutton, David McAllester, Satinder Singh, and Yishay Mansour. Policy gradient methods for reinforcement learning with function approximation. *Advances in neural information processing systems*, 12, 1999.
- Erik Sverdrup, Han Wu, Susan Athey, and Stefan Wager. Qini curves for multi-armed treatment rules. *Journal of Computational and Graphical Statistics*, pages 1–13, 2024.
- Eric J Tchetgen Tchetgen and Tyler J VanderWeele. On causal inference in the presence of interference. *Statistical Methods in Medical Research*, 21(1):55–75, 2012.
- Aleksey Tetenov. Statistical treatment choice based on asymmetric minimax regret criteria. *Journal of Econometrics*, 166(1):157–165, 2012. doi: <https://doi.org/10.1016/j.jeconom.2011.06.013>.
- A. W. van der Vaart. *Asymptotic Statistics*. Cambridge Series in Statistical and Probabilistic Mathematics. Cambridge University Press, 1998.
- Benjamin Van Roy. *Learning and Value Function Approximation in Complex Decision Processes*. PhD thesis, Massachusetts Institute of Technology, 1998.
- Davide Viviano. Policy targeting under network interference. *Review of Economic Studies*, page rdae041, 2024.
- Stefan Wager and Susan Athey. Estimation and inference of heterogeneous treatment effects using random forests. *Journal of the American Statistical Association*, 113(523):1228–1242, 2018.
- Martin J. Wainwright. *High-Dimensional Statistics: A Non-Asymptotic Viewpoint*. Cambridge Series in Statistical and Probabilistic Mathematics. Cambridge University Press, 2019.

- Jia Wan, Sean R Sinclair, Devavrat Shah, and Martin J Wainwright. Exploiting exogenous structure for sample-efficient reinforcement learning. *arXiv preprint arXiv:2409.14557*, 2024.
- Yuanjia Wang, Haoda Fu, and Donglin Zeng. Learning optimal personalized treatment rules in consideration of benefit and risk: with an application to treating type 2 diabetes patients with insulin therapies. *Journal of the American Statistical Association*, 113(521): 1–13, 2018.
- Kuang Xu and Carri W Chan. Using future information to reduce waiting times in the emergency department via diversion. *Manufacturing & Service Operations Management*, 18(3):314–331, 2016.
- Yizhe Xu, Tom H Greene, Adam P Bress, Brian C Sauer, Brandon K Bellows, Yue Zhang, William S Weintraub, Andrew E Moran, and Jincheng Shen. Estimating the optimal individualized treatment rule from a cost-effectiveness perspective. *Biometrics*, 78(1): 337–351, 2022.
- Steve Yadowsky, Scott Fleming, Nigam Shah, Emma Brunskill, and Stefan Wager. Evaluating treatment prioritization rules via rank-weighted average treatment effects. *Journal of the American Statistical Association*, 120(549):38–51, 2025.
- Nur Hani Zainal, Robert M. Bossarte, Sarah M. Gildea, Irving Hwang, Chris J. Kennedy, Howard Liu, Alex Luedtke, Brian P. Marx, Maria V. Petukhova, Edward P. Post, Eric L. Ross, Nancy A. Sampson, Erik Sverdrup, Brett Turner, Stefan Wager, and Ronald C. Kessler. Developing an individualized treatment rule for veterans with major depressive disorder using electronic health records. *Molecular Psychiatry*, 29(8):2335–2345, 2024.
- Ruohan Zhan, Shichao Han, Yuchen Hu, and Zhenling Jiang. Estimating treatment effects under recommender interference: A structured neural networks approach. *arXiv preprint arXiv:2406.14380*, 2024.
- Baqun Zhang, Anastasios A Tsiatis, Eric B Laber, and Marie Davidian. Robust estimation of optimal dynamic treatment regimes for sequential treatment decisions. *Biometrika*, 100(3):681–694, 2013.
- Yi Zhang and Kosuke Imai. Individualized policy evaluation and learning under clustered network interference. *arXiv preprint arXiv:2311.02467*, 2023.
- Yiming Zhang and Keith W Ross. On-policy deep reinforcement learning for the average-reward criterion. In *International Conference on Machine Learning*, pages 12535–12545. PMLR, 2021.
- Zhengyuan Zhou, Susan Athey, and Stefan Wager. Offline multi-action policy learning: Generalization and optimization. *Operations Research*, 71(1):148–183, 2023.

Supplemental Materials

A Closed Forms of Transition Kernels and Stationary Distributions

In this section, we derive the closed forms of transition kernels and stationary distributions for the queuing processes discussed in the paper. We start with the transition kernel and stationary distribution of the embedded point process recorded at both arrivals and services corresponding to the $M_n/M/1$ system discussed in Section 3.3, of which the standard $M/M/1$ system is a special case. We then show that it is possible to find the stationary distribution of the embedded point process recorded only at arrivals using the stationary distribution of the embedded point process recorded at both arrivals and services. Finally, we derive the closed forms of transition kernels of the parallel queuing system discussed in Section 3.2, which provides foundation for approximating its stationary distribution computationally.

A.1 Transition Kernel and Stationary Distribution of an $M_n/M/1$ system

For the embedded point process recorded at both arrivals and services, the state contains both the event type A and the queue length K . Given the current queue length, event type, and treatment assignment, the queue length observed at the next event is deterministic, and the next event type is independent of the history given the queue length observed at the next event, with

$$f_A|_K(a|k) = \begin{cases} \lambda_k I(k < \bar{k}) / (\lambda_k I(k < \bar{k}) + \mu I(k > 0)) & \text{if } a = 1 \\ \mu I(k > 0) / (\lambda_k I(k < \bar{k}) + \mu I(k > 0)) & \text{if } a = 0. \end{cases} \quad (\text{S1})$$

Let $\bar{\pi}(s) = \mathbb{E}[\pi(X_i, S_i) | S_i = s]$. We note that the system's transition kernel under policy π , defined as $P_S^\pi(s' | s) := \bar{\pi}(k)P_S(s' | s, 1) + (1 - \bar{\pi}(k))P_S(s' | s, 0)$, can be expressed as follows:

$$P_S^\pi(a', k' | a, k) = \begin{cases} \bar{\pi}(k)f_A|_K(a' | k+1) & \text{if } a = 1, k' = k+1 \\ (1 - \bar{\pi}(k))f_A|_K(a' | k) & \text{if } a = 1, k' = k \\ f_A|_K(a' | k-1) & \text{if } a = 0, k' = k-1 \\ 0, & \text{otherwise.} \end{cases} \quad (\text{S2})$$

To compute the stationary distribution $d_\pi(a, k)$, notice that the next event type is sampled independently of the past given the queue length. This allows us to first focus on the dynamics of the queue lengths only and derive $d^\dagger(k)$. $d(a, k)$ could then be computed as

$$d(a, k) = d^\dagger(k) \cdot f_A|_K(a | k) \quad (\text{S3})$$

Since the number of states is finite, solving the corresponding system of equations to obtain the stationary distribution is straightforward, with

$$d^\dagger(k) = \frac{r_k}{\sum_{m=0}^{\bar{k}} r_k}, \quad k = 0, \dots, \bar{k}, \quad (\text{S4})$$

and

$$\begin{aligned}
r_0 &= 1 \\
r_1 &= \frac{(\lambda_1 + \mu)\bar{\pi}_0}{\mu} \\
r_k &= \frac{(\lambda_k + \mu)\bar{\pi}_0}{\mu} \prod_{m=1}^{k-1} \frac{\lambda_m \bar{\pi}_m}{\mu}, \quad k = 2, \dots, \bar{k} - 1, \\
r_{\bar{k}} &= \bar{\pi}_0 \prod_{m=1}^{\bar{k}-1} \frac{\lambda_m \bar{\pi}_m}{\mu}.
\end{aligned} \tag{S5}$$

A.2 Stationary Distribution of Embedded Point Process Recorded at Arrivals

To find the stationary distribution of the embedded point process recorded only at arrivals, we note that this process conditions in addition that the event is an arrival. Thus, its stationary distribution could be expressed and computed as

$$\begin{aligned}
\mathbb{P}_\pi [K = k \mid A = 1] &= \frac{\mathbb{P}_\pi [K = k, A = 1]}{\sum_{k'=0}^{\bar{k}} \mathbb{P}_\pi [K = k', A = 1]} \\
&= \frac{d(1, k)}{\sum_{k'=0}^{\bar{k}} d(1, k')}.
\end{aligned} \tag{S6}$$

A.3 Parallel Queue with Routing

Let the state be (A, K_0, K_1) where $A = 0$ and $A = 1$ represent service at queue 0 and queue 1, respectively, and $A = 2$ represent arrival. We write down the transition kernel corresponding to the setting where there is no maximum capacity of queue 0, as considered in the numerical example in Section 4.2:

$$P_S(a', k'_0, k'_1 \mid 2, k_0, k_1, w) = \begin{cases} f_A|_{K_0, K_1}(a' \mid k'_0, k'_1) & \text{if } k'_0 = k_0 + 1, k'_1 = k_1, w = 0 \\ f_A|_{K_0, K_1}(a' \mid k'_0, k'_1) & \text{if } k'_0 = k_0, k'_1 = k_1 + 1, w = 1 \\ 0, & \text{otherwise,} \end{cases}$$

$$P_S(a', k'_0, k'_1 \mid 0, k_0, k_1, w) = \begin{cases} f_A|_{K_0, K_1}(a' \mid k'_0, k'_1) & \text{if } k'_0 = k_0 - 1, k'_1 = k_1, k_0 > 0 \\ 0, & \text{otherwise,} \end{cases}$$

and

$$P_S(a', k'_0, k'_1 \mid 1, k_0, k_1, w) = \begin{cases} f_A|_{K_0, K_1}(a' \mid k'_0, k'_1) & \text{if } k'_0 = k_0, k'_1 = k_1 - 1, k_1 > 0 \\ 0, & \text{otherwise,} \end{cases}$$

where

$$f_A|_{K_0, K_1}(a \mid k_0, k_1) = \begin{cases} \tilde{\lambda}/(\tilde{\lambda} + \mu_0 I(k_0 > 0) + \mu_1 I(k_1 > 0)) & \text{if } a = 2 \\ \mu_0 I(k_0 > 0)/(\tilde{\lambda} + \mu_0 I(k_0 > 0) + \mu_1 I(k_1 > 0)) & \text{if } a = 0 \\ \mu_1 I(k_1 > 0)/(\tilde{\lambda} + \mu_0 I(k_0 > 0) + \mu_1 I(k_1 > 0)) & \text{if } a = 1, \end{cases}$$

and $\tilde{\lambda} = \lambda \cdot I(k_0 \leq \bar{k}_0 \text{ or } k_1 \leq \bar{k}_1)$. The system's transition kernel under policy π can be thus expressed as follows:

$$P_S^\pi(a', k'_0, k'_1 | a, k_0, k_1) = \begin{cases} \bar{\pi}(k_0, k_1) f_A(a' | k_0, k_1 + 1) & \text{if } a = 2, k'_0 = k_0, k'_1 = k_1 + 1 \\ (1 - \bar{\pi}(k_0, k_1)) f_A(a' | k_0 + 1, k_1) & \text{if } a = 2, k'_0 = k_0 + 1, k'_1 = k_1 \\ f_A(a' | k_0, k_1 - 1) & \text{if } a = 1, k'_0 = k_0, k'_1 = k_1 - 1, k_1 > 0 \\ f_A(a' | k_0 - 1, k_1) & \text{if } a = 0, k'_0 = k_0 - 1, k'_1 = k_1, k_0 > 0 \\ 0, & \text{otherwise.} \end{cases}$$

B Proof of Theorems, Propositions, and Corollaries

B.1 Proof of Proposition 1

Define the differential Q-function and value function under policy π as

$$Q_\pi(x, s, w) = \lim_{n \rightarrow \infty} \mathbb{E}_\pi \left[\sum_{i=1}^n (Y_i - \mu(\pi)) \mid X_1 = x, S_1 = s, W_1 = w \right] \quad (\text{S7})$$

and

$$V_\pi(x, s) = \lim_{n \rightarrow \infty} \mathbb{E}_\pi \left[\sum_{i=1}^n (Y_i - \mu(\pi)) \mid X_1 = x, S_1 = s \right]. \quad (\text{S8})$$

It is well known that the following Bellman equation holds for any pairs of differential Q-functions and value functions [Sutton and Barto, 2018].

Lemma 9. *Consider the tuple (X, S, W, Y, X', S') . Under Assumptions 1 and 2, the following Bellman equations hold:*

$$Q_\pi(X, S, W) + \mu(\pi) = \mathbb{E} [Y + V_\pi(X', S') \mid X, S, W]. \quad (\text{S9})$$

For notational simplicity, we sometimes abuse notation and write $\mathbb{P} [W_i = w \mid X_i = x, S_i = s] = \pi_w(x, s)$, $w = 0, 1$. Note that, for any $\tilde{\pi}$,

$$\begin{aligned} \frac{\partial}{\partial \tilde{\pi}} V_\pi(x, s) &= \frac{\partial}{\partial \tilde{\pi}} \sum_w \pi_w(x, s) Q_\pi(x, s, w) \\ &= \sum_w \frac{\partial \pi_w(x, s)}{\partial \tilde{\pi}} Q_\pi(x, s, w) + \sum_w \pi_w(x, s) \frac{\partial Q_\pi(x, s, w)}{\partial \tilde{\pi}} \\ &= \sum_w \frac{\partial \pi_w(x, s)}{\partial \tilde{\pi}} Q_\pi(x, s, w) - \sum_w \pi_w(x, s) \frac{\partial \mu(\pi)}{\partial \tilde{\pi}} \\ &\quad + \int_{\mathcal{X}} \sum_{w, s'} \pi_w(x, s) P_S(s' \mid s, w) P_X(x') \frac{\partial V_\pi(x', s')}{\partial \tilde{\pi}} dx', \end{aligned} \quad (\text{S10})$$

where the last equality follows by applying Lemma 9. Multiplying both sides with $d_\pi(s) P_X(x)$

and integrating over (x, s) gives

$$\begin{aligned}
\frac{\partial \mu(\pi)}{\partial \tilde{\pi}} &= \int_{\mathcal{X}} \sum_s d_{\pi}(s) P_X(x) \sum_w \frac{\partial \pi_w(x, s)}{\partial \tilde{\pi}} Q_{\pi}(x, s, w) \, dx \\
&\quad - \int_{\mathcal{X}} \sum_s d_{\pi}(s) P_X(x) \frac{\partial V_{\pi}(x, s)}{\partial \tilde{\pi}} \, dx \\
&\quad + \sum_s d_{\pi}(s) \int_{\mathcal{X}} \sum_{w, s'} \pi_w(x, s) P_S(s' | s, w) P_X(x') \frac{\partial V_{\pi}(x', s')}{\partial \tilde{\pi}} \, dx' \\
&= \int_{\mathcal{X}} \sum_s d_{\pi}(s) P_X(x) \sum_w \frac{\partial \pi_w(x, s)}{\partial \tilde{\pi}} Q_{\pi}(x, s, w) \, dx \\
&\quad - \int_{\mathcal{X}} \sum_s d_{\pi}(s) P_X(x) \frac{\partial V_{\pi}(x, s)}{\partial \tilde{\pi}} \, dx \\
&\quad + \int_{\mathcal{X}} \sum_s d_{\pi}(s) P_X(x) \frac{\partial V_{\pi}(x, s)}{\partial \tilde{\pi}} \, dx \\
&= \int_{\mathcal{X}} \sum_s d_{\pi}(s) P_X(x) \sum_w \frac{\partial \pi_w(x, s)}{\partial \tilde{\pi}} Q_{\pi}(x, s, w) \, dx.
\end{aligned} \tag{S11}$$

Taking $\tilde{\pi}$ to be $\pi(x, s)$ yields that

$$\begin{aligned}
\frac{\partial}{\partial \pi(x, s)} \mu(\pi) &= d_{\pi}(s) P_X(x) \{Q_{\pi}(x, s, 1) - Q_{\pi}(x, s, 0)\} \\
&= d_{\pi}(s) P_X(x) \{\tau(x, s) + C_{\pi}(s)\}.
\end{aligned} \tag{S12}$$

B.2 Proof of Theorem 2

To isolate the policy taken at a specific coordinate of interest (x, s) from the rest of the policy, we expand our notation of the policy gradient to explicitly depend on the treatment assignment probability at (x, s) . For the purpose of the proof, in this subsection, we will write

$$H(p_{x,s}, \pi) = \frac{1}{P_X(x) \cdot d_{p_{x,s}, \pi}(s)} \frac{\partial}{\partial p_{x,s}} \mu(p_{x,s}, \pi), \tag{S13}$$

where $(p_{x,s}, \pi)$ denotes the policy that takes the value $p_{x,s}$ at the coordinate (x, s) and follows $\pi(x', s')$ for $(x', s') \neq (x, s)$.

For all fixed pairs of (x, s) , since $p_{x,s} \in [0, 1]$, $p_{x,s}^*$, the treatment assignment probability at (x, s) that optimizes $\mu(p_{x,s}, \pi)$, must satisfy one of the following three conditions:

$$H(p_{x,s}^*, \pi) = 0, \quad p_{x,s}^* \in [0, 1], \tag{S14}$$

$$H(p_{x,s}^*, \pi) > 0, \quad p_{x,s}^* = 1, \tag{S15}$$

and

$$H(p_{x,s}^*, \pi) < 0, \quad p_{x,s}^* = 0, \tag{S16}$$

for all π' .

From Proposition 1,

$$H(p_{x,s}^*, \pi) = \tau(x, s) + C_{p_{x,s}^*, \pi}(s). \tag{S17}$$

where $C_{p_{x,s}^*, \pi}(s)$ is a finite constant that only varies across s for all fixed π . Thus, Conditions (S15) and (S16) are equivalent to

$$p_{x,s}^* = I(H(p_{x,s}^*, \pi) > 0) = I(\tau(x, s) > -C_{p_{x,s}^*, \pi}(s)). \quad (\text{S18})$$

Furthermore, Condition (S14) is equivalent to

$$p_{x,s}^* = I(\tau(x, s) = -C_{p_{x,s}^*, \pi}(s)) \cdot p_{x,s}^*, \quad (\text{S19})$$

for some $p_{x,s}^* \in [0, 1]$.

Now we show that, for all x that the condition $\tau(x, s) = -C_{p_{x,s}^*, \pi}(s)$ is satisfied, it is possible to find some $p_s \in [0, 1]$ such that the objective remains the same if we set $p_{x,s}^* = p_s$ for those x . We begin by proving the following Lemma.

Lemma 10. *Under Assumptions of Theorem 2, for $x_1, x_2 \in \mathcal{X}$ and $s \in \mathcal{S}$ such that $\tau(x_1, s) = \tau(x_2, s)$,*

$$\mu(p_{x_1, s}, p_{x_2, s}, \pi) = \mu(p'_{x_1, s}, p'_{x_2, s}, \pi) \quad (\text{S20})$$

if $P_X(x_1)p_{x_1, s} + P_X(x_2)p_{x_2, s} = P_X(x_1)p'_{x_1, s} + P_X(x_2)p'_{x_2, s}$, where $(p_{x_1, s}, p_{x_2, s}, \pi)$ denotes the policy that takes the value $p_{x_1, s}$ and $p_{x_2, s}$ at the coordinates (x_1, s) and (x_2, s) , and follows $\pi(x', s')$ for $(x', s') \neq (x_1, s), (x_2, s)$.

Lemma 10 implies that it suffices to only differentiate between treatment probabilities where the CATE is different for a fixed state. Since the CADE always equals to $-C_{p_{x,s}^*, \pi}(s)$ when Condition (S14) is met, there must exists some $p_s \in [0, 1]$ where

$$p_{x,s}^* = p_s \in \arg \max_{p_{x,s}} \mu(p_{x,s}, \pi^*), \quad \pi^* \in \arg \max_{\pi} \mu(p_s, \pi^*) \quad (\text{S21})$$

for all x such that $\tau(x, s) = -C_{p_{x,s}^*, \pi}(s)$. Taking $c_s = -C_{p_{x,s}^*, \pi^*}(s)$ establishes the first part of the theorem.

To prove the second part of the theorem, simply notice that when $\tau(X, s)$ is continuous for all s ,

$$\mathbb{P}[\tau(X, s) = -C_{p_{X,s}^*, \pi}(s)] = 0, \quad (\text{S22})$$

and thus it suffices to consider only the last two conditions.

B.3 Proof of Theorem 3

To start with, we show that, for any two different policies, the difference in policy values can be controlled by two factors: the discrepancy in conditional average treatment effects, and the difference between the threshold values. Recall that we will use $\bar{\pi}(s) = \mathbb{E}[\pi(X_i, s)]$ we denote the probability of assigning treatment at state s .

Lemma 11. *Under the assumptions of Theorem 3, for any two policies π, π' such that*

$$\pi(x, s) = I(\tau(x, s) > c_s), \quad \pi'(x, s) = I(\tau'(x, s) > c'_s), \quad (\text{S23})$$

$\forall x \in \mathcal{X}, s \in \mathcal{S}$, the difference between their policy values can be bounded as

$$|\mu(\pi) - \mu(\pi')| \lesssim \left(\max_s \|\tau(X_i, s) - \tau'(X_i, s)\|_{L_2(P_X)} \right)^{\frac{2}{3}} + \|c - c'\|_{\infty}. \quad (\text{S24})$$

It follows directly from Lemma 11 and the assumption (13) that

$$|\mu(\hat{\pi}) - \mu(\pi^*)| \lesssim \mathcal{O}_p\left(n^{-\frac{2\beta}{3}}\right) + \|\hat{c} - c^*\|_\infty. \quad (\text{S25})$$

Now we find a bound for $\|\hat{c} - c^*\|_\infty$. For all s ,

$$\hat{c}_s = \kappa_{1-\hat{g}_s}(\hat{\tau}(X_i, s)), \quad (\text{S26})$$

where

$$\hat{g}_s \in \operatorname{argmax}_g \hat{\mu}(\pi_{\hat{\tau},g}). \quad (\text{S27})$$

We first bound $|\hat{g}_s - g_s^*|$. This requires bounding

$$\begin{aligned} \sup_g |\hat{\mu}(\pi_{\hat{\tau},g}) - \mu(\pi_{\tau,g})| \\ \leq \sup_g |\hat{\mu}(\pi_{\hat{\tau},g}) - \mu(\pi_{\hat{\tau},g})| + \sup_g |\mu(\pi_{\hat{\tau},g}) - \mu(\pi_{\tau,g})|. \end{aligned} \quad (\text{S28})$$

Recall that $\hat{\tau}$ is obtained out-of-sample and thus can be considered fixed, and thus a bound on the first term follows directly from the condition (14). To bound the second term of (S28), by Lemma 11 and condition (13),

$$\sup_g |\mu(\pi_{\hat{\tau},g}) - \mu(\pi_{\tau,g})| \lesssim \mathcal{O}_p\left(n^{-\frac{2\beta}{3}}\right). \quad (\text{S29})$$

The proof of the following lemma is similar to that of the consistency of an M-estimator [van der Vaart, 1998].

Lemma 12. *Under the assumptions of Theorem 3, for all $s \in \mathcal{S}$,*

$$|\hat{g}_s - g_s^*| = \mathcal{O}_p\left(n^{-\frac{2\beta}{3}} + n^{-\gamma}\right). \quad (\text{S30})$$

Next, we bound $|\hat{c}_s - c_s^*|$, which equals

$$\begin{aligned} |\hat{c}_s - c_s^*| &= |\kappa_{1-\hat{g}_s}(\hat{\tau}(X_i, s)) - \kappa_{1-g_s^*}(\tau(X_i, s))| \\ &\leq |\kappa_{1-\hat{g}_s}(\hat{\tau}(X_i, s)) - \kappa_{1-\hat{g}_s}(\tau(X_i, s))| \\ &\quad + |\kappa_{1-\hat{g}_s}(\tau(X_i, s)) - \kappa_{1-g_s^*}(\tau(X_i, s))|. \end{aligned} \quad (\text{S31})$$

From Assumption 3, $\tau(X_i, s)$ has a density that is bounded from below. As a result, the quantile function $\kappa_g(\tau(X_i, s))$ is differentiable almost everywhere with derivative bounded above by the reciprocal of the lower bound of the density. This suggests that $\kappa_g(\tau(X_i, s))$ is Lipschitz continuous in g , and thus the second term in (S31) can be bounded as

$$\begin{aligned} |\kappa_{1-\hat{g}_s}(\tau(X_i, s)) - \kappa_{1-g_s^*}(\tau(X_i, s))| &\leq \mathcal{O}(|\hat{g}_s - g_s^*|) \\ &= \mathcal{O}_p\left(n^{-\frac{2\beta}{3}} + n^{-\gamma}\right). \end{aligned} \quad (\text{S32})$$

To bound the first term in (S31), note that

$$\begin{aligned} |\kappa_{1-\hat{g}_s}(\hat{\tau}(X_i, s)) - \kappa_{1-\hat{g}_s}(\tau(X_i, s))| &\leq W_1(\hat{\tau}(X_i, s), \tau(X_i, s)) \\ &\leq \|\hat{\tau}(X_i, s) - \tau(X_i, s)\|_{L_2(P_X)} \\ &= \mathcal{O}(n^{-\beta}), \end{aligned} \quad (\text{S33})$$

where $W_1(\hat{\tau}(X_i, s), \tau(X_i, s))$ is the Wasserstein-1 distance $\hat{\tau}(X_i, s)$ and $\tau(X_i, s)$. Putting everything together yields that

$$\begin{aligned} |\mu(\hat{\pi}) - \mu(\pi^*)| &\lesssim \mathcal{O}_p\left(n^{-\frac{2\beta}{3}}\right) + \|\hat{c} - c^*\|_\infty \\ &= \mathcal{O}_p\left(n^{-\frac{2\beta}{3}}\right) + \mathcal{O}_p\left(n^{-\frac{2\beta}{3}} + n^{-\gamma}\right) + \mathcal{O}\left(n^{-\beta}\right) \\ &= \mathcal{O}_p\left(n^{-\frac{2\beta}{3}}\right) + \mathcal{O}_p\left(n^{-\gamma}\right). \end{aligned} \quad (\text{S34})$$

B.4 Proof of Proposition 4

When a sup-norm bound on the estimated CATE function is available, it is possible to derive an alternative bound on the difference in policy values, where the discrepancy in treatment effects is also controlled in the sup-norm rather than the L_2 -norm.

Lemma 13. *Under the assumptions of Proposition 4, for any two policies π, π' such that*

$$\pi(x, s) = I(\tau(x, s) > c_s), \quad \pi'(x, s) = I(\tau'(x, s) > c'_s), \quad (\text{S35})$$

$\forall x \in \mathcal{X}, s \in \mathcal{S}$, the difference between their policy values can be bounded as

$$|\mu(\pi) - \mu(\pi')| \lesssim \|\tau - \tau'\|_\infty + \|c - c'\|_\infty. \quad (\text{S36})$$

Plugging in $\hat{\pi}$ and π^* yields that

$$|\mu(\hat{\pi}) - \mu(\pi^*)| \lesssim \mathcal{O}_p\left(n^{-\beta}\right) + \|\hat{c} - c^*\|_\infty. \quad (\text{S37})$$

Again, to bound $\|\hat{c} - c^*\|_\infty$, we start by bounding

$$\begin{aligned} \sup_g |\hat{\mu}(\pi_{\hat{\tau}, g}) - \mu(\pi_{\tau, g})| \\ \leq \sup_g |\hat{\mu}(\pi_{\hat{\tau}, g}) - \mu(\pi_{\hat{\tau}, g})| + \sup_g |\mu(\pi_{\hat{\tau}, g}) - \mu(\pi_{\tau, g})|. \end{aligned} \quad (\text{S38})$$

A bound on the first term still follows directly from the condition (14). To bound the second term of (S38), by Lemma 13 and condition (17),

$$\sup_g |\mu(\pi_{\hat{\tau}, g}) - \mu(\pi_{\tau, g})| \lesssim \mathcal{O}_p\left(n^{-\beta}\right). \quad (\text{S39})$$

It then follows from the same proof of Lemma 12 that

$$|\hat{g}_s - g_s^*| = \mathcal{O}_p\left(n^{-\beta} + n^{-\gamma}\right), \quad (\text{S40})$$

and thus

$$\|\hat{c} - c^*\|_\infty = \mathcal{O}_p\left(n^{-\beta} + n^{-\gamma}\right). \quad (\text{S41})$$

B.5 Proof of Corollary 7

We denote for shorthand that $\bar{R}(\pi) = \mathbb{E}_\pi[R_i]$ and $\bar{\Delta}(\pi) = \mathbb{E}_\pi[\Delta_i]$. From Lemma 8 and applying chain rule,

$$\begin{aligned} \frac{\partial}{\partial \pi(x, k)} \theta(\pi) &= \frac{\partial}{\partial \pi(x, k)} \frac{\bar{R}(\pi)}{\bar{\Delta}(\pi)} \\ &= \frac{1}{\bar{\Delta}(\pi)^2} \left(\frac{\partial}{\partial \pi(x, k)} \bar{R}(\pi) - \frac{\partial}{\partial \pi(x, k)} \bar{\Delta}(\pi) \right). \end{aligned} \quad (\text{S42})$$

Define the differential Q-function and value function for reward under policy π as

$$Q_{\pi, R}(x, k, w) = \lim_{t \rightarrow \infty} \mathbb{E}_\pi \left[\sum_{i=1}^{N(t)} (R_i - \bar{R}(\pi)) \mid X_1 = x, K_1 = k, W_1 = w \right] \quad (\text{S43})$$

and

$$V_{\pi, R}(x, k) = \lim_{t \rightarrow \infty} \mathbb{E}_\pi \left[\sum_{i=1}^{N(t)} (R_i - \bar{R}(\pi)) \mid X_1 = x, K_1 = k \right], \quad (\text{S44})$$

and similarly, the differential Q-function and value function for interarrival time under policy π as

$$Q_{\pi, \Delta}(x, k, w) = \lim_{t \rightarrow \infty} \mathbb{E}_\pi \left[\sum_{i=1}^{N(t)} (\Delta_i - \bar{\Delta}(\pi)) \mid X_1 = x, K_1 = k \right]. \quad (\text{S45})$$

and

$$V_{\pi, \Delta}(x, k) = \lim_{t \rightarrow \infty} \mathbb{E}_\pi \left[\sum_{i=1}^{N(t)} (\Delta_i - \bar{\Delta}(\pi)) \mid X_1 = x, K_1 = k, W_1 = w \right]. \quad (\text{S46})$$

Below, we show that the Bellman equation holds for the pairs of differential Q-functions and value functions.

Lemma 14. *Consider the tuple $(X, S, W, \Delta, R, X', S')$. Under Assumptions in Corollary 7, the following Bellman equations hold for all π :*

$$\begin{aligned} Q_{\pi, R}(X, S, W) + \bar{R}(\pi) &= \mathbb{E} [R + V_{\pi, R}(X', S') \mid X, S, W], \\ Q_{\pi, \Delta}(X, S, W) + \bar{\Delta}(\pi) &= \mathbb{E} [\Delta + V_{\pi, \Delta}(X', S') \mid X, S, W]. \end{aligned} \quad (\text{S47})$$

Thus, by following the same reasoning as in the proof of Proposition 1,

$$\frac{\partial}{\partial \pi(x, k)} \bar{R}(\pi) = d_\pi(k) P_X(x) \{Q_{\pi, R}(x, k, 1) - Q_{\pi, R}(x, k, 0)\}, \quad (\text{S48})$$

where by Lemma 14,

$$\begin{aligned}
& Q_{\pi,R}(x, k, 1) - Q_{\pi,R}(x, k, 0) \\
&= \mathbb{E} [R_1 \mid X_1 = x, K_1 = k, W_1 = 1] - \mathbb{E} [R_1 \mid X_1 = x, K_1 = k, W_1 = 0] \\
&\quad + \lim_{t \rightarrow \infty} \mathbb{E}_{\pi} \left[\sum_{i=2}^{N(t)} (R_i - \bar{R}(\pi)) \mid K_1 = k, W_1 = 1 \right] \\
&\quad - \lim_{t \rightarrow \infty} \mathbb{E}_{\pi} \left[\sum_{i=2}^{N(t)} (R_i - \bar{R}(\pi)) \mid K_1 = k, W_1 = 0 \right].
\end{aligned} \tag{S49}$$

Similarly, we can get

$$\frac{\partial}{\partial \pi(x, k)} \bar{\Delta}(\pi) = d_{\pi}(k) P_X(x) \{Q_{\pi,\Delta}(x, k, 1) - Q_{\pi,\Delta}(x, k, 0)\}, \tag{S50}$$

and

$$\begin{aligned}
& Q_{\pi,\Delta}(x, k, 1) - Q_{\pi,\Delta}(x, k, 0) \\
&= \lim_{t \rightarrow \infty} \mathbb{E}_{\pi} \left[\sum_{i=2}^{N(t)} (\Delta_i - \bar{\Delta}(\pi)) \mid K_1 = k, W_1 = 1 \right] \\
&\quad - \lim_{t \rightarrow \infty} \mathbb{E}_{\pi} \left[\sum_{i=2}^{N(t)} (\Delta_i - \bar{\Delta}(\pi)) \mid K_1 = k, W_1 = 0 \right].
\end{aligned} \tag{S51}$$

Putting everything together,

$$\begin{aligned}
\frac{\partial}{\partial \pi(x, k)} \theta(\pi) &= \frac{1}{\bar{\Delta}(\pi)^2} \left(\frac{\partial}{\partial \pi(x, k)} \bar{R}(\pi) - \frac{\partial}{\partial \pi(x, k)} \bar{\Delta}(\pi) \right) \\
&= \underbrace{\frac{\tau_{\text{DE},R}(x, k)}{\bar{\Delta}(\pi)}}_{\text{direct effect}} + \underbrace{\frac{\tau_{\text{IE},R}(k; \pi)}{\bar{\Delta}(\pi)}}_{\text{indirect effect through affecting others' outcomes}} \\
&\quad + \underbrace{-\theta(\pi) \cdot \frac{\tau_{\text{IE},\Delta}(k; \pi)}{\bar{\Delta}(\pi)}}_{\text{indirect effect through affecting others' arrivals}}
\end{aligned} \tag{S52}$$

where

$$\tau_{\text{DE},R}(x, k) = \mathbb{E} [R_1 \mid X_1 = x, K_1 = k, W_1 = w] - \mathbb{E} [R_1 \mid X_1 = x, K_1 = k, W_1 = w], \tag{S53}$$

$$\begin{aligned}
\tau_{\text{IE},R}(k; \pi) &= \mathbb{E}_{\pi} \left[\sum_{i=2}^{N(t)} (R_i - \bar{R}(\pi)) \mid K_1 = k, W_1 = 1 \right] \\
&\quad - \mathbb{E}_{\pi} \left[\sum_{i=2}^{N(t)} (R_i - \bar{R}(\pi)) \mid K_1 = k, W_1 = 0 \right],
\end{aligned} \tag{S54}$$

and

$$\begin{aligned} \tau_{\text{IE}, \Delta}(k; \pi) = \mathbb{E}_\pi \left[\sum_{i=2}^{N(t)} (\Delta_i - \bar{\Delta}(\pi)) \mid K_1 = k, W_1 = 1 \right] \\ - \mathbb{E}_\pi \left[\sum_{i=2}^{N(t)} (\Delta_i - \bar{\Delta}(\pi)) \mid K_1 = k, W_1 = 0 \right]. \end{aligned} \quad (\text{S55})$$

The desired result then follows directly from applying the same argument as in the proof of Theorem 2.

C Proof of Lemmas

Proof of Lemma 5. Let's start by considering the estimators

$$\hat{r}_\pi^\dagger(k) := \frac{1}{n_k} \sum_{i=1}^{n_k} \left[\hat{\eta}_\pi(X_i^k, k) + \frac{\pi_{W_i^k}(X_i^k, k)}{\hat{\pi}_{0, W_i^k}(X_i^k, k)} \cdot (Y_i^k - \hat{\eta}(W_i^k, X_i^k, k)) \right] \quad (\text{S56})$$

and

$$\tilde{r}_\pi^\dagger(k) := \frac{1}{n_k} \sum_{i=1}^{n_k} \left[\eta_\pi(X_i^k, k) + \frac{\pi_{W_i^k}(X_i^k, k)}{\pi_{0, W_i^k}(X_i^k, k)} \cdot (Y_i^k - \eta(W_i^k, X_i^k, k)) \right], \quad (\text{S57})$$

where n_k is set to be $\lfloor d_{\pi_0}(k) \cdot n \rfloor$, and X_i^k , W_i^k , and Y_i^k refers to the values of X_i , W_i , and Y_i corresponding to the n_k indices for which $K_i = k$, in order of their occurrence.

For a policy π that sets $\pi(x, k) = I(\tau(x, k) > \kappa_{1-g_k}(\tau(X_i, k)))$ with some $g_k \in [0, 1]$, the estimators can be written explicitly in g_k as

$$\hat{r}_\pi^\dagger(k) := \frac{1}{n_k} \sum_{i=1}^{n_k} f_{g_k}^k(X_i^k, W_i^k, Y_i^k; \hat{\pi}_0, \hat{\eta})$$

and

$$\tilde{r}_\pi^\dagger(k) := \frac{1}{n_k} \sum_{i=1}^{n_k} f_{g_k}^k(X_i^k, W_i^k, Y_i^k; \pi_0, \eta),$$

where

$$\begin{aligned} f_{g_k}^k(x, w, y; \pi_0, \eta) &= \eta_\pi(x, k) + \frac{\pi_{\tau, g_k, w}(x, k)}{\pi_{0, w}(x, k)} \cdot (y - \eta(w, x, k)), \\ \pi_w^{\tau, g_k}(x, k) &= w I(\tau(x, k) > \kappa_{1-g_k}(\tau(x, k))) + (1 - w) I(\tau(x, k) \leq \kappa_{1-g_k}(\tau(x, k))). \end{aligned}$$

We show first that

$$\sup_g \left| \tilde{r}_{\pi_{\tau, g}}^\dagger(k) - r_{\pi_{\tau, g}}(k) \right| = \mathcal{O}_p(n^{-1/2}) \quad (\text{S58})$$

for all fixed states $k \in \mathcal{K}$ and CATE functions $\tau : \mathcal{X} \times \mathcal{K} \rightarrow \mathbb{R}$. To do so, we note that $\tilde{r}_\pi^\dagger(k)$ can be regarded as a sample average of n_k i.i.d. observations, whose expectations all equal to $r_\pi(k)$. Furthermore, since the process regenerates every time it hits state k , the observations taken into account can be considered i.i.d. drawn from the joint stationary distribution under policy π_0 when $K_i = k$.

Lemma 15. *Under assumptions of Lemma 5, for all states k and policies π ,*

$$\mathbb{E}_{\pi_0} [f_{g_k}^k(X_i^k, W_i^k, Y_i^k; \pi_0, \eta)] = r_\pi(k). \quad (\text{S59})$$

Define the Rademacher complexity of the function class

$$\mathcal{F}^k := \{f_{g_k}^k(x, w, y; \pi_0, \eta) : g_k \in (0, 1)\}$$

as

$$R_n(\mathcal{F}^k) = \mathbb{E}_{\pi_0} \left[\mathbb{E}_\epsilon \left[\sup_{f \in \mathcal{F}^k} \left| \frac{1}{n_k} \sum_{i=1}^{n_k} \epsilon_i f(X_i^k, W_i^k, Y_i^k; \pi_0, \eta) \right| \right] \right], \quad (\text{S60})$$

where ϵ_i are i.i.d. random variables uniformly distributed over $\{-1, +1\}$. Below, we show that the Rademacher complexity of the function class \mathcal{F}^k is of order $1/\sqrt{n}$.

Lemma 16. *Under assumptions of Lemma 5, for all state k and policies π ,*

$$R_n(\mathcal{F}^k) = \mathcal{O}(n^{-1/2}). \quad (\text{S61})$$

By standard uniform convergence results based on Rademacher complexity (see, e.g., Chapter 4 of [Wainwright \[2019\]](#)), we have

$$\begin{aligned} & \sup_g \left| \hat{r}_{\pi_{\tau,g}}^\dagger(k) - r_{\pi_{\tau,g}}(k) \right| \\ &= \sup_{f \in \mathcal{F}^k} \left| \frac{1}{n_k} \sum_{i=1}^{n_k} f(X_i^k, W_i^k, Y_i^k; \pi_0, \eta) - \mathbb{E}[f(X_i^k, W_i^k, Y_i^k; \pi_0, \eta)] \right| \\ &= \mathcal{O}_p(R_n(\mathcal{F}^k)) = \mathcal{O}_p(n^{-1/2}). \end{aligned} \quad (\text{S62})$$

Next, we show that

$$\sup_g \left| \hat{r}_{\pi_{\tau,g}}^\dagger(k) - \tilde{r}_{\pi_{\tau,g}}^\dagger(k) \right| = \mathcal{O}_p(n^{-1/2}), \quad (\text{S63})$$

i.e., the error introduced by estimating the nuisances $\hat{\pi}_0$ and $\hat{\eta}$ is small enough. As the other doubly robust estimators, we show that $\hat{r}_{\pi_{\tau,g}}^\dagger(k) - \tilde{r}_{\pi_{\tau,g}}^\dagger(k)$ is a sample average of n_k i.i.d. observations whose expectation could be expressed in a crossed-term form, which is of order $\mathcal{O}(n^{-1/2})$ by Assumption 6.

Lemma 17. *Under assumptions of Lemma 5, for all states k and policies π ,*

$$\begin{aligned} & \mathbb{E}_{\pi_0} [f_{g_k}^k(X_i^k, W_i^k, Y_i^k; \pi_0, \eta) - f_{g_k}^k(X_i^k, W_i^k, Y_i^k; \hat{\pi}_0, \hat{\eta})] \\ &= \mathbb{E}_{\pi_0} \left[\left(\frac{\pi_{W_i^k}(X_i^k, k)}{\pi_{0, W_i^k}(X_i^k, k)} \right) \left(1 - \frac{\pi_{0, W_i^k}(X_i^k, k)}{\hat{\pi}_{0, W_i^k}(X_i^k, k)} \right) \cdot \{\eta(W_i^k, X_i^k, k) - \hat{\eta}(W_i^k, X_i^k, k)\} \right] \\ &= \mathcal{O}_p(n^{-1/2}) \end{aligned}$$

Through a similar Rademacher complexity argument, we show that the uniform convergence rate of $\hat{r}_{\pi_{\tau,g}}^\dagger(k) - \tilde{r}_{\pi_{\tau,g}}^\dagger(k)$ is small.

Lemma 18. *Under assumptions of Lemma 5, for all states k and policies π ,*

$$\sup_g \left| \hat{r}_{\pi_{\tau,g}}^\dagger(k) - \tilde{r}_{\pi_{\tau,g}}^\dagger(k) \right| = \mathcal{O}_p(n^{-1/2}).$$

Finally, we connect $\sup_g \left| \hat{r}_{\pi_{\tau,g}}(k) - r_{\pi_{\tau,g}}(k) \right|$ with the error terms $\sup_g \left| \tilde{r}_{\pi_{\tau,g}}^\dagger(k) - r_{\pi_{\tau,g}}(k) \right|$ and $\sup_g \left| \hat{r}_{\pi_{\tau,g}}^\dagger(k) - \tilde{r}_{\pi_{\tau,g}}^\dagger(k) \right|$ we have bounded. Let $N_k = \sum_{i=1}^{N(T)} I(K_i = k)$. Then

$$\begin{aligned} & \sup_g \left| \hat{r}_{\pi_{\tau,g}}(k) - r_{\pi_{\tau,g}}(k) \right| \\ & \leq \sup_g \left| \hat{r}_{\pi_{\tau,g}}^\dagger(k) - r_{\pi_{\tau,g}}(k) \right| \cdot \left| \frac{n_k}{N_k} \right| \\ & \quad + \sup_f \left| \frac{1}{N_k} \sum_{i=n_k+1}^{N_k} (f(X_i^k, W_i^k, R_i^k; \hat{\pi}_0, \hat{\eta}) - \mathbb{E}[(X_i^k, W_i^k, R_i^k; \pi_0, \eta)]) \right| \cdot I(N_s \geq n_s + 1), \end{aligned}$$

where the first term can be bounded as

$$\begin{aligned} & \sup_g \left| \hat{r}_{\pi_{\tau,g}}^\dagger(k) - r_{\pi_{\tau,g}}(k) \right| \cdot \left| \frac{n_k}{N_k} \right| \\ & \leq \left(\sup_g \left| \tilde{r}_{\pi_{\tau,g}}^\dagger(k) - r_{\pi_{\tau,g}}(k) \right| + \sup_g \left| \hat{r}_{\pi_{\tau,g}}^\dagger(k) - \tilde{r}_{\pi_{\tau,g}}^\dagger(k) \right| \right) \cdot \left| \frac{n_k}{N_k} \right| \\ & = \mathcal{O}_p\left(\frac{1}{\sqrt{n}}\right), \end{aligned}$$

and the second term is of smaller order.

To verify the uniform convergence rate of $\hat{\mu}(\pi)$, note that

$$\begin{aligned} \sup_g |\hat{\mu}(\pi_{\tau,g}) - \mu(\pi_{\tau,g})| &= \sup_g \left| \sum_k \hat{r}_{\pi_{\tau,g}}(k) \hat{d}_\pi(k) - \sum_k r_\pi(k) d_\pi(k) \right| \\ &\leq \sum_k \sup_g \left| \hat{r}_\pi(k) \hat{d}_\pi(k) - r_\pi(k) d_\pi(k) \right| \\ &\leq \sum_{k,w} \hat{r}_\pi(k) \cdot \sup_g \left| \hat{d}_\pi(k) - d_\pi(k) \right| + \sum_k d_\pi(k) \cdot \sup_g |\hat{r}_\pi(k) - r_\pi(k)| \end{aligned} \tag{S64}$$

Since $\hat{r}_\pi(k)$ is bounded almost surely, it remains to show that $\sup_g \left| \hat{d}_\pi(k) - d_\pi(k) \right| = \mathcal{O}_p(1/\sqrt{n})$, which follows directly from the assumptions on the estimation of λ and μ .

Lemma 19. *Under assumptions of Lemma 5, for all states k and policies π ,*

$$\sup_g \left| \hat{d}_\pi(k) - d_\pi(k) \right| = \mathcal{O}_p(n^{-1/2}).$$

□

Proof of Lemma 10. For the two policies $(p_{x_1,s}, p_{x_2,s}, \pi)$ and $(p'_{x_1,s}, p'_{x_2,s}, \pi)$,

$$\begin{aligned} & \mu(p_{x_1,s}, p_{x_2,s}, \pi) - \mu(p'_{x_1,s}, p'_{x_2,s}, \pi) \\ &= \sum_{s \in \mathcal{S}} d_{p_{x_1,s}, p_{x_2,s}, \pi}(s) \{P_X(x_1)p_{x_1,s}\tau(x_1, s) + P_X(x_2)p_{x_2,s}\tau(x_2, s)\} \\ & \quad - \sum_{s \in \mathcal{S}} d_{p'_{x_1,s}, p'_{x_2,s}, \pi}(s) \{P_X(x_1)p'_{x_1,s}\tau(x_1, s) + P_X(x_2)p'_{x_2,s}\tau(x_2, s)\} \end{aligned} \quad (\text{S65})$$

Note that the transition kernel induced by a policy π can be written as

$$P_S^\pi(s' | s) = \int_{\mathcal{X}} P_X(x) \{P_S(s' | s, 1)\pi(x, s) + P_S(s' | s, 0)(1 - \pi(x, s))\} dx. \quad (\text{S66})$$

Thus, $d_{p_{x_1,s}, p_{x_2,s}, \pi}(s) = d_{p'_{x_1,s}, p'_{x_2,s}, \pi}(s)$ as long as

$$\begin{aligned} & P_S^{p_{x_1,s}, p_{x_2,s}, \pi}(s' | s) - P_S^{p'_{x_1,s}, p'_{x_2,s}, \pi}(s' | s) \\ &= P_X(x_1) \{ (P_S(s' | s, 1) - P_S(s' | s, 0)) (p_{x_1,s} - p'_{x_1,s}) \} \\ & \quad + P_X(x_2) \{ (P_S(s' | s, 1) - P_S(s' | s, 0)) (p_{x_2,s} - p'_{x_2,s}) \} \\ &= \{ P_S(s' | s, 1) - P_S(s' | s, 0) \} \\ & \quad \cdot \{ P_X(x_1) (p_{x_1,s} - p'_{x_1,s}) + P_X(x_2) (p_{x_2,s} - p'_{x_2,s}) \} \\ &= 0 \end{aligned} \quad (\text{S67})$$

for all s' .

When equation (S67) holds, (S65) becomes

$$\begin{aligned} (\text{S65}) &= \sum_{s \in \mathcal{S}} d_{p_{x_1,s}, p_{x_2,s}, \pi}(s) P_X(x_1) \tau(x_1, s) [p_{x_1,s} - p'_{x_1,s}] \\ & \quad + \sum_{s \in \mathcal{S}} d_{p_{x_1,s}, p_{x_2,s}, \pi}(s) P_X(x_2) \tau(x_2, s) [p_{x_2,s} - p'_{x_2,s}] \\ &= \sum_{s \in \mathcal{S}} d_{p_{x_1,s}, p_{x_2,s}, \pi}(s) \tau(x_1, s) \\ & \quad \cdot \{ P_X(x_1) (p_{x_1,s} - p'_{x_1,s}) + P_X(x_2) (p_{x_2,s} - p'_{x_2,s}) \}, \end{aligned} \quad (\text{S68})$$

which equals zero if $P_X(x_1) (p_{x_1,s} - p'_{x_1,s}) + P_X(x_2) (p_{x_2,s} - p'_{x_2,s}) = 0$. □

Proof of Lemma 11. First, we note that

$$\begin{aligned} |\mu(\pi) - \mu(\pi')| &= |\mathbb{E}_\pi[Y_i] - \mathbb{E}_{\pi'}[Y_i]| \\ &= \left| \sum_{s,w} \int_{\mathcal{X}} \mathbb{E}[Y_i | W_i = w, S_i = s, X_i = x] \cdot P_X(x) \cdot d_\pi(s) \right. \\ & \quad \cdot I(\tau(x, s) > c_s) (2w - 1) dx \\ & \quad \left. - \sum_{s,w} \int_{\mathcal{X}} \mathbb{E}[Y_i | W_i = w, S_i = s, X_i = x] \cdot P_X(x) \cdot d_{\pi'}(s) \right| \end{aligned}$$

$$\begin{aligned}
& \cdot [I(\tau'(x, s) > c'_s) (2w - 1)] dx \\
& \lesssim |\mathbb{E}_\pi [I(\tau(X_i, S_i) > c_{S_i}) - I(\tau'(X_i, S_i) > c'_{S_i})]| \quad (\text{S69}) \\
& \quad + \max_s |d_\pi(s) - d_{\pi'}(s)|. \quad (\text{S70})
\end{aligned}$$

We start by bounding (S69), the error due to the mismatch in distributions of W_i when S_i is always from $d_\pi(\cdot)$:

$$\begin{aligned}
(\text{S69}) & \lesssim \max_s |\mathbb{E} [I(\tau(X_i, s) > c_s) - I(\tau'(X_i, s) > c'_s)]| \\
& \leq \max_s |\mathbb{E} [I(\tau(X_i, s) > c'_s) - I(\tau'(X_i, s) > c'_s)]| \quad (\text{S71})
\end{aligned}$$

$$+ \max_s |\mathbb{E} [I(\tau(X_i, s) > c_s) - I(\tau(X_i, s) > c'_s)]|. \quad (\text{S72})$$

To bound (S71), note that for all c'_s and any $\epsilon > 0$,

$$\begin{aligned}
(\text{S71}) & = \max_s \mathbb{E} [I(\pi(X_i, s) \neq \pi'(X_i, s))] \\
& \leq \max_s \mathbb{E} [I(\pi(X_i, s) \neq \pi'(X_i, s)) \cdot I(|\tau(X_i, s) - c_s| \leq \epsilon)] \\
& \quad + \max_s \mathbb{E} [I(\pi^*(X_i, s) \neq \hat{\pi}(X_i, s)) \cdot I(|\tau(X_i, s) - c_s| > \epsilon)] \\
& \leq \max_s \mathbb{E} [I(|\tau(X_i, s) - c_s| \leq \epsilon)] \quad (\text{S73}) \\
& \quad + \max_s \mathbb{E} [I(\tau(X_i, s) \neq \tau'(X_i, s)) \cdot I(|\tau(X_i, s) - \tau'(X_i, s)| > \epsilon)] \\
& \leq \max_s \mathbb{P} [|\tau(X_i, s) - c_s| \leq \epsilon] + \max_s \frac{\|\tau(X_i, s) - \tau'(X_i, s)\|_{L_2(P_X)}^2}{\epsilon^2},
\end{aligned}$$

where the third inequality follows from Markov's inequality. From Assumption 3, $\tau(X_i, s)$ has a density that is bounded from above. As a result, for all state s ,

$$\mathbb{P} [|\tau(X_i, s) - c_s| \leq \epsilon] = \mathcal{O}(\epsilon). \quad (\text{S74})$$

Combining this result with the Jensen's inequality yields that

$$(\text{S71}) \lesssim \epsilon + \frac{\left(\max_s \|\tau(X_i, s) - \tau'(X_i, s)\|_{L_2(P_X)} \right)^2}{\epsilon^2}. \quad (\text{S75})$$

Taking

$$\epsilon = \left(\max_s \|\tau(X_i, s) - \tau'(X_i, s)\|_{L_2(P_X)} \right)^{\frac{2}{3}}, \quad (\text{S76})$$

there is

$$(\text{S71}) \lesssim \left(\max_s \|\tau(X_i, s) - \tau'(X_i, s)\|_{L_2(P_X)} \right)^{\frac{2}{3}}. \quad (\text{S77})$$

To bound (S72), notice that

$$\begin{aligned}
(\text{S72}) & \leq \max_s \mathbb{P} [|\tau(X_i, s) - c_s| \leq \|c - c'\|_\infty] \\
& \lesssim \|c - c'\|_\infty. \quad (\text{S78})
\end{aligned}$$

Putting everything together yields that

$$(S69) \lesssim \left(\max_s \|\tau(X_i, s) - \tau'(X_i, s)\|_{L_2(P_X)} \right)^{\frac{2}{3}} + \|c - c'\|_\infty. \quad (S79)$$

Now it remains to bound (S70). It follows from Assumption 4 that

$$\begin{aligned} (S70) &\lesssim \|\bar{\pi} - \bar{\pi}'\|_\infty \\ &= \max_s |\mathbb{E} [\pi(X_i, s) - \pi'(X_i, s)]| \\ &= \max_s |\mathbb{E} [I(\tau(X_i, s) > c_s) - I(\tau'(X_i, s) > c'_s)]|, \end{aligned} \quad (S80)$$

which is again of the same order as (S69). Putting everything together yields the claimed result. \square

Proof of Lemma 12. By (15) and (S28),

$$\begin{aligned} \hat{\mu}(\pi_{\hat{\tau}, \hat{g}}) &\geq \hat{\mu}(\pi_{\hat{\tau}, g^*}) - \mathcal{O}_p(T^{-\frac{2\beta}{3}} + T^{-\gamma}) \\ &\geq \mu(\pi_{\tau, g^*}) - \mathcal{O}_p(T^{-\frac{2\beta}{3}} + T^{-\gamma}). \end{aligned} \quad (S81)$$

Thus, by (S28),

$$\begin{aligned} \mu(\pi_{\tau, g^*}) - \mu(\pi_{\tau, \hat{g}}) &\leq \hat{\mu}(\pi_{\hat{\tau}, \hat{g}}) - \mu(\pi_{\tau, \hat{g}}) + \mathcal{O}_p(T^{-\frac{2\beta}{3}} + T^{-\gamma}) \\ &= \mathcal{O}_p(T^{-\frac{2\beta}{3}} + T^{-\gamma}). \end{aligned} \quad (S82)$$

Combining this with Assumption 5 yields that $|\hat{g}_s - g_s^*| = \mathcal{O}_p(T^{-\frac{2\beta}{3}} + T^{-\gamma})$. \square

Proof of Lemma 13. From Lemma 11,

$$|\mu(\pi) - \mu(\pi')| \lesssim \max_s |\mathbb{E} [I(\tau(X_i, s) > c_s) - I(\tau'(X_i, s) > c'_s)]|. \quad (S83)$$

To bound (S83), note that

$$\begin{aligned} (S83) &\leq \max_s \mathbb{P} [|\tau(X_i, s) - c_s| \leq |\tau(X_i, s) - \tau'(X_i, s)| + \|c - c'\|_\infty] \\ &\lesssim \|\tau - \tau'\|_\infty + \|c - c'\|_\infty. \end{aligned} \quad (S84)$$

\square

Proof of Lemma 15. Note that

$$\begin{aligned} &\mathbb{E}_{\pi_0} \left[\frac{\pi_{W_i^k}(X_i^k, k)}{\pi_{0, W_i^k}(X_i^k, k)} \cdot Y_i^k \right] \\ &= \mathbb{E}_{\pi_0} \left[\frac{\pi_{W_i}(X_i, k)}{\pi_{0, W_i}(X_i, k)} \cdot Y_i \mid K_i = k \right] \\ &= \sum_w \int_{\mathcal{X}} P_X(x) \pi_{0, w}(x, k) \frac{\pi_w(x, k)}{\pi_{0, w}(x, k)} \cdot \mathbb{E} [Y_i \mid K_i = k, W_i = w, X_i = x] dx \\ &= \sum_w \int_{\mathcal{X}} P_X(x) \pi_w(x, k) \cdot \mathbb{E} [Y_i \mid K_i = k, W_i = w, X_i = x] dx \\ &= r_\pi(k). \end{aligned} \quad (S85)$$

Similarly,

$$\begin{aligned}
& \mathbb{E}_{\pi_0} \left[\eta_{\pi}(X_i^k, k) - \frac{\pi_{W_i^k}(X_i^k, k)}{\pi_{0, W_i^k}(X_i^k, k)} \cdot \eta(W_i^k, X_i^k, k) \right] \\
&= \mathbb{E} [\eta_{\pi}(X_i, k)] - \mathbb{E}_{\pi_0} \left[\frac{\pi_{W_i}(X_i, k)}{\pi_{0, W_i}(X_i, k)} \cdot \eta(W_i, X_i, k) \mid K_i = k \right] \\
&= \mathbb{E} [\eta_{\pi}(X_i, k)] - \mathbb{E}_{\pi} [\eta(W_i, X_i, k)] \\
&= 0.
\end{aligned} \tag{S86}$$

Thus,

$$\mathbb{E}_{\pi_0} \left[\eta_{\pi}(X_i^k, k) + \frac{\pi_{W_i^k}(X_i^k, k)}{\pi_{0, W_i^k}(X_i^k, k)} \cdot (Y_i^k - \eta(W_i^k, X_i^k, k)) \right] = r_{\pi}(k). \tag{S87}$$

□

Proof of Lemma 16. To start with, consider the function $h_{g_k}^k : \mathcal{X} \times \{0, 1\} \times \mathbb{R} \mapsto \mathbb{R}^4$, with

$$\begin{aligned}
h_{1, g_k}^k(x, w, y) &= wI(\tau(x, k) > \kappa_{1-g_k}(\tau(X_i, k))), \\
h_{2, g_k}^k(x, w, y) &= (1-w)I(\tau(x, k) \leq \kappa_{1-g_k}(\tau(X_i, k))), \\
h_{3, g_k}^k(x, w, y) &= \frac{1}{\pi_{0, w}(x, k)} \cdot (y - \eta(W_i, X_i, k)), \\
h_{4, g_k}^k(x, w, y) &= \eta_{\pi}(x, k)
\end{aligned} \tag{S88}$$

Note that $f_{g_k}^k(x, w, y)$ can be written as

$$f_{g_k}^k(x, w, y) = (h_{1, g_k}^k(x, w, y) + h_{2, g_k}^k(x, w, y))h_{3, g_k}^k(x, w, y) + h_{4, g_k}^k(x, w, y). \tag{S89}$$

Since $\pi_{0, w}(x, k)$ is bounded away from zero for all (x, k) , $f_{g_k}^k(x, w, y)$ is a Lipschitz function of $h_{j, g_k}^k(x, w, y)$. By the contraction inequality of Lipschitz functions with vector-valued domains [Maurer, 2016],

$$R_n(\mathcal{F}^k) \lesssim \sum_{j=1}^4 R_n(\mathcal{H}_j^k), \quad \mathcal{H}_j^k := \{h_{j, g_k}^k : g_k \in (0, 1)\}. \tag{S90}$$

We start by analyzing the class \mathcal{H}_1^k (and the same argument applies to \mathcal{H}_2^k). The functions in \mathcal{H}_1^k correspond to threshold functions when $W_i = 1$, which have VC dimension 1, and are identically zero when $W_i = 0$. Thus, the Rademacher complexity of \mathcal{H}_1^k is of order $1/\sqrt{n_s}$. \mathcal{H}_3^k and \mathcal{H}_4^k are just singleton classes with zero complexity. Thus,

$$R_n(\mathcal{F}^k) = \mathcal{O}(n_s^{-1/2}) = \mathcal{O}(n^{-1/2}). \tag{S91}$$

□

Proof of Lemma 17. Note that

$$\mathbb{E} [\eta_{\pi}(X_i^k, k)] = \mathbb{E}_{\pi_0} \left[\frac{\pi_{W_i^k}(X_i^k, k)}{\pi_{0, W_i^k}(X_i^k, k)} \cdot \eta(W_i^k, X_i^k, k) \right]. \tag{S92}$$

Thus,

$$\begin{aligned}
& \mathbb{E}_{\pi_0} [f_{g_k}^k(X_i^k, W_i^k, Y_i^k; \pi_0, \eta) - f_{g_k}^k(X_i^k, W_i^k, Y_i^k; \hat{\pi}_0, \hat{\eta})] \\
&= \mathbb{E} [\eta_\pi(X_i^k, k) - \hat{\eta}_\pi(X_i^k, k)] + \mathbb{E}_{\pi_0} \left[\left(\frac{\pi_{W_i^k}(X_i^k, k)}{\pi_{0, W_i^k}(X_i^k, k)} - \frac{\pi_{W_i^k}(X_i^k, k)}{\hat{\pi}_{0, W_i^k}(X_i^k, k)} \right) \cdot Y_i^k \right] \\
&\quad - \mathbb{E}_{\pi_0} \left[\frac{\pi_{W_i^k}(X_i^k, k)}{\pi_{0, W_i^k}(X_i^k, k)} \cdot \eta(W_i^k, X_i^k, k) - \frac{\pi_{W_i^k}(X_i^k, k)}{\hat{\pi}_{0, W_i^k}(X_i^k, k)} \cdot \hat{\eta}(W_i^k, X_i^k, k) \right] \\
&= -\mathbb{E} [\hat{\eta}_\pi(X_i^k, k)] + \mathbb{E}_{\pi_0} \left[\left(\frac{\pi_{W_i^k}(X_i^k, k)}{\pi_{0, W_i^k}(X_i^k, k)} \right) \left(1 - \frac{\pi_{0, W_i^k}(X_i^k, k)}{\hat{\pi}_{0, W_i^k}(X_i^k, k)} \right) \cdot Y_i^k \right] \\
&\quad + \mathbb{E}_{\pi_0} \left[\frac{\pi_{W_i^k}(X_i^k, k)}{\hat{\pi}_{0, W_i^k}(X_i^k, k)} \cdot \hat{\eta}(W_i^k, X_i^k, k) \right] \\
&= -\mathbb{E}_{\pi_0} \left[\frac{\pi_{W_i^k}(X_i^k, k)}{\pi_{0, W_i^k}(X_i^k, k)} \hat{\eta}(W_i^k, X_i^k, k) \right] + \mathbb{E}_{\pi_0} \left[\frac{\pi_{W_i^k}(X_i^k, k)}{\hat{\pi}_{0, W_i^k}(X_i^k, k)} \cdot \hat{\eta}(W_i^k, X_i^k, k) \right] \\
&\quad + \mathbb{E}_{\pi_0} \left[\left(\frac{\pi_{W_i^k}(X_i^k, k)}{\pi_{0, W_i^k}(X_i^k, k)} \right) \left(1 - \frac{\pi_{0, W_i^k}(X_i^k, k)}{\hat{\pi}_{0, W_i^k}(X_i^k, k)} \right) \cdot Y_i^k \right] \\
&= -\mathbb{E}_{\pi_0} \left[\left(\frac{\pi_{W_i^k}(X_i^k, k)}{\pi_{0, W_i^k}(X_i^k, k)} \right) \left(1 - \frac{\pi_{0, W_i^k}(X_i^k, k)}{\hat{\pi}_{0, W_i^k}(X_i^k, k)} \right) \cdot \hat{\eta}(W_i^k, X_i^k, k) \right] \\
&\quad + \mathbb{E}_{\pi_0} \left[\left(\frac{\pi_{W_i^k}(X_i^k, k)}{\pi_{0, W_i^k}(X_i^k, k)} \right) \left(1 - \frac{\pi_{0, W_i^k}(X_i^k, k)}{\hat{\pi}_{0, W_i^k}(X_i^k, k)} \right) \cdot \eta(W_i^k, X_i^k, k) \right] \\
&= \mathbb{E}_{\pi_0} \left[\left(\frac{\pi_{W_i^k}(X_i^k, k)}{\pi_{0, W_i^k}(X_i^k, k)} \right) \left(1 - \frac{\pi_{0, W_i^k}(X_i^k, k)}{\hat{\pi}_{0, W_i^k}(X_i^k, k)} \right) \cdot \{ \eta(W_i^k, X_i^k, k) - \hat{\eta}(W_i^k, X_i^k, k) \} \right].
\end{aligned}$$

□

Proof of Lemma 18. We start by noticing that, by Lemma 17,

$$\begin{aligned}
& \sup_g \left| \hat{r}_{\pi_{\tau, g}}^\dagger(k) - \tilde{r}_{\pi_{\tau, g}}^\dagger(k) \right| \\
&= \sup_g \left| \hat{r}_{\pi_{\tau, g}}^\dagger(k) - \tilde{r}_{\pi_{\tau, g}}^\dagger(k) - \mathbb{E}_{\pi_0} [f_{g_k}^k(X_i^k, W_i^k, Y_i^k; \pi_0, \eta) - f_{g_k}^k(X_i^k, W_i^k, Y_i^k; \hat{\pi}_0, \hat{\eta})] \right| \\
&\quad + \mathbb{E}_{\pi_0} [f_{g_k}^k(X_i^k, W_i^k, Y_i^k; \pi_0, \eta) - f_{g_k}^k(X_i^k, W_i^k, Y_i^k; \hat{\pi}_0, \hat{\eta})] \\
&= \sup_g \left| \hat{r}_{\pi_{\tau, g}}^\dagger(k) - \tilde{r}_{\pi_{\tau, g}}^\dagger(k) - \mathbb{E}_{\pi_0} [f_{g_k}^k(X_i^k, W_i^k, Y_i^k; \pi_0, \eta) - f_{g_k}^k(X_i^k, W_i^k, Y_i^k; \hat{\pi}_0, \hat{\eta})] \right| + \mathcal{O}(n^{-1/2}).
\end{aligned}$$

To find $\sup_g \left| \hat{r}_{\pi_{\tau, g}}^\dagger(k) - \tilde{r}_{\pi_{\tau, g}}^\dagger(k) - \mathbb{E}_{\pi_0} [f_{g_k}^k(X_i^k, W_i^k, Y_i^k; \pi_0, \eta) - f_{g_k}^k(X_i^k, W_i^k, Y_i^k; \hat{\pi}_0, \hat{\eta})] \right|$, we need to find the Rademacher complexity of the function class

$$\{ f_{g_k}^k(x, w, y; \pi_0, \eta) - f_{g_k}^k(x, w, y; \hat{\pi}_0, \hat{\eta}) : g_k \in (0, 1) \},$$

where $f_{g_k}^k(x, w, y; \pi_0, \eta) - f_{g_k}^k(x, w, y; \hat{\pi}_0, \hat{\eta})$ can be written as

$$(h_{1, g_k}^k(x, w, y) + h_{2, g_k}^k(x, w, y)) \cdot (\tilde{h}_{3, g_k}^k(x, w, y) + \tilde{h}_{4, g_k}^k(x, w, y)), \quad (\text{S93})$$

with $h_{1,g_k}^k(x, w, y)$ and $h_{2,g_k}^k(x, w, y)$ defined as in the proof of Lemma 16, and

$$\begin{aligned}\tilde{h}_{3,g_k}^k(x, w, y) &= \frac{1}{\pi_{0,w}(x, k)} \cdot (y - \eta(W_i, X_i, k)) - \frac{1}{\hat{\pi}_{0,w}(x, k)} \cdot (y - \hat{\eta}(W_i, X_i, k)), \\ \tilde{h}_{4,g_k}^k(x, w, y) &= \eta(w, x, k) - \hat{\eta}(w, x, k).\end{aligned}\tag{S94}$$

Since $\hat{\pi}_0$ and $\hat{\eta}$ are obtained out-of-sample and not affected by the choice of g , the function classes composed of $\tilde{h}_{3,g_k}^k(x, w, y)$ and $\tilde{h}_{4,g_k}^k(x, w, y)$ are singleton classes with zero complexity, and the Rademacher complexity of the function class

$$\{f_{g_k}^k(x, w, y; \pi_0, \eta) - f_{g_k}^k(x, w, y; \hat{\pi}_0, \hat{\eta}) : g_k \in (0, 1)\}$$

is $\mathcal{O}(n^{-1/2})$. Thus,

$$\begin{aligned}\sup_g \left| \hat{r}_{\pi_{\tau,g}}^\dagger(k) - \tilde{r}_{\pi_{\tau,g}}^\dagger(k) \right| \\ = \sup_g \left| \hat{r}_{\pi_{\tau,g}}^\dagger(k) - \tilde{r}_{\pi_{\tau,g}}^\dagger(k) - \mathbb{E}_{\pi_0} [f_{g_k}^k(X_i^k, W_i^k, Y_i^k; \pi_0, \eta) - f_{g_k}^k(X_i^k, W_i^k, Y_i^k; \hat{\pi}_0, \hat{\eta})] \right| + \mathcal{O}(n^{-1/2}) \\ = \mathcal{O}_p(n^{-1/2}).\end{aligned}$$

□

Proof of Lemma 19. Recall that $\hat{d}_\pi(k)$ is a plug-in estimator of $d_\pi(k)$ obtained by substituting λ and μ with their respective estimates $\hat{\lambda}$ and $\hat{\mu}$. From Section A, $d_\pi(k)$ can be written a Lipschitz function of λ and μ over all choices of $\bar{\pi}_{k'} = g_{k'} \in (0, 1)$, $k' = 1, \dots, \bar{k}$. Thus, it follows directly that

$$\sup_g \left| \hat{d}_\pi(k) - d_\pi(k) \right| = \mathcal{O}_p \left(\left| \hat{\lambda} - \lambda \right| + |\hat{\mu} - \mu| \right) = \mathcal{O}_p \left(n^{-1/2} \right)$$

□